

Longitudinal coupling between electrically driven spin-qubits and a resonator

Sarath Prem,^{1,*} Marcin M. Wysokiński,¹ and Mircea Trif¹

¹*International Research Centre MagTop, Institute of Physics, Polish Academy of Sciences,
Aleja Lotników 32/46, PL-02668 Warsaw, Poland*

(Dated: January 25, 2023)

At the core of the semiconducting spin qubits success is the ability to manipulate them electrically, enabled by the spin-orbit interactions. However, most implementations require external magnetic fields to define the spin qubit, which in turn activate various charge noise mechanisms. Here we study spin qubits confined in quantum dots at zero magnetic fields, that are driven periodically by electrical fields and are coupled to a microwave resonator. Using Floquet theory, we identify a well-defined Floquet spin-qubit originating from the lowest degenerate spin states in the absence of driving. We find both transverse and longitudinal couplings between the Floquet spin qubit and the resonator, which can be selectively activated by modifying the driving frequency. We show how these couplings can facilitate fast qubit readout and the implementation of a two-qubit CPHASE gate. Finally, we use adiabatic perturbation theory to demonstrate that the spin-photon couplings originate from the non-Abelian geometry of states endowed by the spin-orbit interactions, rendering these findings general and applicable to a wide range of solid-state spin qubits.

I. INTRODUCTION

Solid-state systems based quantum bits (qubits) have seen tremendous progress in the last decades.^{1,2} Among the solid-state platforms, electron and holes spins localised in semiconductor quantum dots (QDs) have been at the forefront of research because of their long coherence times, scalability, and a natural compatibility with industrial-grade semiconductor manufacturing technologies.^{3–8} Fast and high-fidelity readout,^{9,10} single-qubit control,^{11–13} and two-qubit logic^{14–16} have been demonstrated in different experiments.

One of the main ingredients that have accelerated the advances in spin-qubit implementations is the strong spin-orbit interaction (SOI) that electrons and holes experience in semiconductors, as it facilitates their fast manipulation by external electrical fields via the electric dipole spin resonance (EDSR).^{17–21} Furthermore, it enables to interface spins with photons in microwave resonators (or cavities), which allows fast qubit state detection and generation of long-range spin entanglement.^{22,23} The downside of strong SOI, however, is that it exposes the spin to various charge noise sources, leading to a reduced spin qubit coherence, in particular in the presence of an external magnetic field that splits the spin states. While that can be mitigated by operating the qubit at sweet spots where the decoherence is minimised,^{20,24–27} it requires fine tuning of the electrostatic confinements which restricts the parameter phase space where they can be operated.

Driving the spin qubit can enhance its coherence. For example, it was shown recently that by shuttling electrons in an array of 3×3 laterally defined QDs in GaAs heterostructure,²⁸ the coherence time was enhanced by a factor of 10 as compared to stationary QDs. This was because the effect of the hyperfine interactions, which dominate the dephasing in the static GaAs QDs, averages to zero during the dynamics, in analogy to the effect of motional narrowing phenomenon observed in

NMR.^{29,30} Furthermore, recent works have shown that Floquet qubits encoded in the quasi-energy structure occurring in periodically driven superconducting systems can exhibit a larger number of sweet spots for operation that their static counterparts, which facilitates their operation.^{31–33}

Dynamics not only extends the spin qubit coherence, but it also enables its manipulation in the absence of any externally applied magnetic fields (that are used routinely to define the spin qubit). Indeed, as demonstrated in Refs. 34–36, the spin of an electron or hole confined in a QD acquires a non-Abelian geometric phase when it is displaced on closed trajectories by electrical fields in the presence of SOI. It was shown theoretically that by appropriately choosing the QD trajectory, it is possible to implement a universal set of single-qubit gates,³⁷ and even generate entanglement.³⁸ Overall, the geometric spin manipulation is potentially more robust than the resonant EDSR, since it is not affected by gate timing errors and charge noise.^{39–41}

In this paper, we consider the coupling between electrically driven SO coupled QDs hosting electron or hole spins in zero applied magnetic field, and a microwave resonator. Using the Floquet theory appropriate for periodic driving, we identify a well-defined Floquet spin qubit encoded in two of the quasi-energy levels. We unravel a novel longitudinal coupling between the spin qubit driven at frequency Ω and the photons

$$H_{s-p} \propto \Omega \tau_z^F (a^\dagger + a), \quad (1)$$

which occurs in the absence of any applied magnetic field, and is activated when Ω matches the frequency of the resonator. When two such qubits are immersed in the same resonator, we demonstrate that a CPHASE gate can be implemented on fast time scales, in particular for hole-spin qubits. To test its robustness, we use a Floquet-Born-Markov density matrix approach to establish the influence of charge noises, and estimate that the Floquet spin qubits are long-lived. Finally, we show that

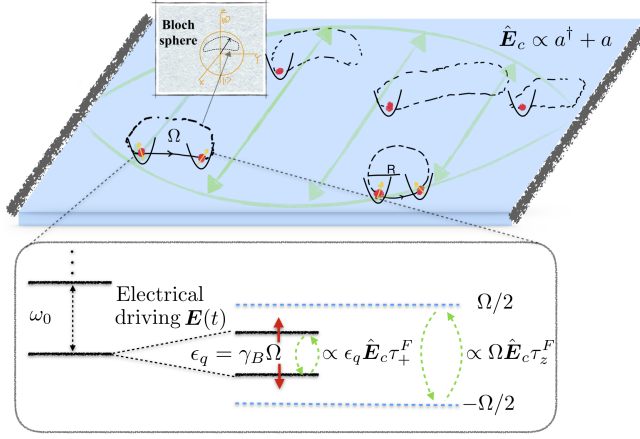


FIG. 1. Schematics of the setup. Several single electron or hole spins confined in QDs with level spacing ω_0 and coupled to the electric field (green arrows) of a microwave resonator. Applying time-dependent electrical fields $\mathbf{E}(t)$ oscillating at a frequency $\Omega \ll \omega_0$, displace the QDs on closed trajectories in the semiconductor, inducing in turn rotations of the lowest degenerate spinors on the Bloch sphere. The Berry phase accumulated during the rotation, γ_B , defines an effective Floquet spin qubit Hamiltonian with a splitting $\epsilon_q \sim \gamma_B \Omega$. The QD dynamics triggers both transverse ($\propto \epsilon_q \hat{\mathbf{E}}_c \tau_+^F$) and longitudinal ($\propto \Omega \hat{\mathbf{E}}_c \tau_z^F$) spin-photon interactions, that are activated for $\omega_c \sim \epsilon_q$ and $\omega_c \sim \Omega$, respectively, allowing to detect the Floquet spin qubit state and entangle remote spins interacting with a common resonator.

the coupling to the photons originates from the electron or hole spin qubits geometry of states endowed by the SOI, rendering our proposal general and applicable to a wide variety of spin-qubit implementations.

The paper is organised as follows: in Sec. II we introduce the model and review the static spin qubits in QDs coupled to a microwave resonator. Then, in Sec. III we use Floquet theory for periodically driven spins by electrical fields, identify the Floquet qubit, and determine its coupling to the resonator. In Sec. IV we show how to readout its state and spectrum with both longitudinal and transverse interactions, while in Sec. V discusses the coherence of the Floquet spin qubits using the Floquet-Born-Markov theory. In Sec. VI we show how to construct a CPHASE two-qubit gate, and estimate its time scales. In Sec. VII we offer a geometrical perspective of the combined dynamics and infer the generality of our findings. Finally, in Sec. VIII we end up with conclusions and an outlook.

II. MODEL AND STATIC RESULTS

For concreteness we apply our dynamical scheme to gate defined QDs, hosting either electrons or holes. A schematics of the system is shown in Fig. 1. It consists of one (or several) electron or hole spins, confined in mobile QDs defined in a two-dimensional semiconductor

and immersed in a common microwave resonator with a fundamental frequency ω_c . Moreover, the QDs are well separated from each other so that there is no tunnelling between them. The Hamiltonian describing one of the QDs ($\hbar = 1$):⁷

$$\begin{aligned} H_{\text{tot}}(t) &= H_0(t) + H_{SO} + H_{e-p} + \omega_c a^\dagger a, \\ H_0(t) &= \frac{\mathbf{p}^2}{2m} + U(\mathbf{r}) + \frac{1}{2}g\mu_B B\sigma_z + e\mathbf{r} \cdot \mathbf{E}(t), \quad (2) \\ H_{SO} &= \alpha(p_x\sigma_y - p_y\sigma_x) + \beta(-p_x\sigma_x + p_y\sigma_y), \\ H_{e-p} &= e\mathbf{r} \cdot \mathbf{E}_c(a^\dagger + a), \end{aligned}$$

where $\mathbf{p} = -i\partial/\partial\mathbf{r}$ is the electron/hole momentum in the QD, B is an external in-plane magnetic field, $\mathbf{E}(t)$ is the classical electrical field acting on the QD, while \mathbf{E}_c is the amplitude of the resonator electric field with annihilation (creation) operator a (a^\dagger). Here, $U(\mathbf{r})$ is the confinement potential, while H_{SO} represents the spin-orbit coupling Hamiltonian accounting for the Rashba ($\propto \alpha$) and Dresselhaus ($\propto \beta$) contributions.⁴² Also, g and μ_B are the g -factor and the Bohr magneton, respectively, while σ_β with $\beta = x, y, z$, are the Pauli matrices acting on the QD electronic spin. Without loss of generality, we assume in the following parabolic confinement potential for each of the dots, i. e. $U(\mathbf{r}) = m\omega_0^2 r^2/2$, where ω_0 is the confining frequency. Consequently, in the presence of the electric fields $U(\mathbf{r}) \rightarrow U[\mathbf{r} - \mathbf{R}(t)]$, with $\mathbf{R}(t) = -e\mathbf{E}(t)/(m\omega_0^2)$, i.e. a shifted confining potential (up to a constant term of no physical relevance). As demonstrated later, more general confining potentials alter quantitatively the resulting Hamiltonians, but retain the same qualitative features. Furthermore, other forms of SOI, such as the cubic-in-momentum⁴² can be easily accounted for within the same formalism.

Next in this section we briefly review the static spin-orbit qubits defined in the presence of a magnetic field. The main purpose of this summary is to establish the benchmark results to be compared against the dynamical cases. Throughout the rest of this section we set $\mathbf{E}(t) = 0$, i. e. the QDs are not electrically driven. In the absence of an external magnetic field the QD energy levels are at least doubly degenerate, consequence of the Kramers theorem. The logical qubit subspace consists of the two lowest eigenstates $\{|\psi_0\rangle, |\psi_1\rangle\}$ of the Hamiltonian $H_d = H_0 + H_{SO}$, with a finite qubit (Zeeman) splitting $E_Z = \epsilon_1 - \epsilon_0$ when the QD is subject to an external magnetic field. The effective qubit-photon interaction is found by projecting the electron-photon Hamiltonian onto the qubit subspace⁴³ which gives (using the identities in Eq. 47 in Appendix A):

$$H_{s-p} = g_+ \tau_+ (a^\dagger + a) + \text{h.c.}, \quad (3)$$

$$g_+ = iE_Z \frac{\mathbf{R}_c}{\lambda_{SO}} \cdot \mathbf{m}_+, \quad (4)$$

where $\mathbf{m}_+ = \langle \psi_0 | \mathbf{m} | \psi_1 \rangle$ with $\mathbf{m} = \lambda_{SO} \boldsymbol{\lambda}_{SO}^{-1} \boldsymbol{\sigma}$, and we defined $\mathbf{R}_c = e\mathbf{E}_c/m\omega_0^2$ as the distance over which the electrical field of the resonator shifts the center of the

QD. Also, τ_γ are the $\gamma = x, y, z$ Pauli matrices acting in the qubit subspace, with $H_s = E_Z \tau_z/2$ defining the qubit Hamiltonian, while $\lambda_{SO}^{-1} = \|\boldsymbol{\lambda}_{SO}^{-1}\|/\sqrt{2}$ represents the Frobenius norm of the SOI matrix.¹⁷ This Hamiltonian can now be scrutinised both close to the resonance with the photons, $\omega_c \sim E_Z$, which reproduces the Jaynes-Cummings Hamiltonian when the counter-rotating terms are neglected, as well as in the dispersive regime, $|g_+| \ll |\omega_c - E_Z|$, that allows to determine the qubit state from the resonator frequency shift.^{7,43} Moreover, when two such qubits are coupled to the same resonator, it induces entangling interactions between the two,^{22,43} that can be used for two-qubit gates construction.

The SOI-induced spin-photon interaction above exhibit two main features. First, it is exact in the SOI, the sole condition being weak electron-photon coupling and $\omega_0 \gg E_Z$. Moreover, it vanishes in the limit $B \rightarrow 0$ and therefore $E_Z \propto B$, again consequence of the Kramers theorem. Second, the coupling is purely transverse ($\propto \tau_{x,y}$) in leading order in the electron-photon coupling, which limits its usefulness. Indeed, a transverse coupling hybridizes the resonator and the spin degrees of freedom, which can result in strong qubit decay (via the Purcell effect) and, moreover, the readout is not truly non-demolition.⁴⁴ While such effects can be mitigated by detuning the qubit strongly from the resonator when compared to $|g_+|$, it also results in a reduction of the effective coupling and it is restricted to a small number of photons in the resonator.²² A longitudinal coupling instead, of the form in Eq. 1, does not suffer of these limitations, and can facilitate the readout of the qubit, as demonstrated in Ref. 45. Furthermore, it allows for fast and high-fidelity two-qubit gates.^{46–48} In the following we turn the discussion to the driven QDs and demonstrate the emergence of such longitudinal terms and how they can be selectively activated.

III. FLOQUET SPIN QUBIT—PHOTON INTERACTIONS

EDSR represents a staple method for manipulating solid-state qubits such as electron or hole spins localized in QDs in the presence of a qubit splitting caused by external (or effective) magnetic fields. Here we scrutinise whether by driving the QDs electrically in the SOI field allows to define, manipulate, and detect them in the absence of any such magnetic fields. Therefore, in this section we set $B = 0$, and switch on the time-dependent electrical fields $\mathbf{E}(t+T) = \mathbf{E}(t)$ acting on a single QD, while in a later section we discuss the implications for several such QDs. The natural theoretical framework to describe the dynamics in this case is the Floquet theory.⁴⁹ The time-dependent Schrodinger equation describing the evolution of the QD in the absence of the resonator is:

$$i\partial_t |\Psi_j(t)\rangle = H_d(t) |\Psi_j(t)\rangle, \quad (5)$$

where $H_d(t) = H_0(t) + H_{SO}$, and the state $|\Psi_j(t)\rangle$, with $j = 0, 1, 2, \dots$, can be expressed as $|\Psi_j(t)\rangle = e^{-i\epsilon_j t} |\psi_j(t)\rangle$, where ϵ_j is the Floquet quasi-energy [defined $\text{mod}(2\pi/T)$], and $|\psi_j(t+T)\rangle = |\psi_j(t)\rangle$ is the periodic component of the Floquet state.⁵⁰ They form therefore a complete basis, defining the unique set of stationary solutions to the Schrodinger equation. The electronic evolution operator reads:

$$U(t, 0) = \sum_j |\psi_j(t)\rangle \langle \psi_j(0)| e^{-i\epsilon_j t}, \quad (6)$$

and, hence, the matrix element of an operator \mathcal{O} of the system in the interaction picture becomes:

$$\mathcal{O}(t) = \sum_{j,j'} \mathcal{O}_{jj'}(t) |\psi_j(0)\rangle \langle \psi_{j'}(0)| e^{i(\epsilon_j - \epsilon_{j'})t}, \quad (7)$$

with $|\psi_j(0)\rangle$ being the Floquet states at time $t = 0$ when the measurement starts and $\mathcal{O}_{jj'}(t) = \langle \psi_j(t) | \mathcal{O} | \psi_{j'}(t) \rangle$. Furthermore, since $\mathcal{O}_{jj'}(t+T) = \mathcal{O}_{jj'}(t)$, we can write $\mathcal{O}_{jj'}(t) = \sum_k \mathcal{O}_{jj'}(k) e^{ik\Omega t}$, with $\mathcal{O}_{jj'}(k)$ the corresponding Fourier component and $\Omega = 2\pi/T$ is the precession frequency. Of particular interest is the position operator, which, as demonstrated in the Appendix A, can be written as:

$$\mathbf{r}_{jj'}(t) = \frac{i}{m\lambda_{SO}} \sum_k \frac{\Delta\epsilon_{jj'} + k\Omega}{\omega_0^2 - (\Delta\epsilon_{jj'} + k\Omega)^2} e^{-ik\Omega t} \mathbf{m}_{jj'}(k),$$

where $\Delta\epsilon_{jj'} = \epsilon_j - \epsilon_{j'}$, and $\mathbf{m}_{jj'}(k)$ is the k -th Fourier component of $\mathbf{m}_{jj'}(t) = \langle \psi_j(t) | \mathbf{m} | \psi_{j'}(t) \rangle$. The above expression readily allows to express the electron-photon interaction Hamiltonian in the Floquet basis states and, moreover, to select the two Floquet levels that describe well a qubit. In this work, we focus on driving frequencies $\Omega \ll \omega_0$, such that the dynamics remains confined within the lowest instantaneous doublet [a more rigorous condition that quantifies the adiabatic regime is given by $|\dot{\mathbf{R}}| \ll \lambda_0 \omega_0$,^{34,35} with $\lambda_0 = \sqrt{1/(m\omega_0)}$ being the QD lateral size]. Therefore, we can pick from the Floquet ladder the ones that originate from this doublet, a choice that we confirm in a later section by using an adiabatic perturbation theory.

Projecting the above expression onto the subspace spanned by the above two Floquet states, $\{|\psi_0(0)\rangle, |\psi_1(0)\rangle\}$, we find:

$$\begin{aligned} H_{s-p}(t) &= [g_z(t) \tau_z^F + (g_+(t) \tau_+^F + \text{h.c.})] (a^\dagger + a) + \omega_c a^\dagger a, \\ g_z(t) &= \frac{\mathbf{R}_c}{2\lambda_{SO}} \cdot \frac{d}{dt} \mathbf{m}_z(t), \\ g_+(t) &= ie^{i\epsilon_q t} \frac{\mathbf{R}_c}{\lambda_{SO}} \cdot \left(\epsilon_q - i \frac{d}{dt} \right) \mathbf{m}_+(t), \end{aligned} \quad (8)$$

where $\boldsymbol{\tau}^F = (\tau_x^F, \tau_y^F, \tau_z^F)$ are Pauli matrices acting in the Floquet subspace spanned by the above states, $\tau_\pm^F = \tau_x^F \pm i\tau_y^F$, and $\epsilon_q = \epsilon_1 - \epsilon_0$ is the Floquet qubit splitting. Also, $\mathbf{m}_z(t) = \langle \psi_1(t) | \mathbf{m} | \psi_1(t) \rangle - \langle \psi_0(t) | \mathbf{m} | \psi_0(t) \rangle$

and $\mathbf{m}_+(t) = \langle \psi_1(t) | \mathbf{m} | \psi_0(t) \rangle$. Eq. 8 constitutes one of our main results: it describes the spin-photon coupling for SO-coupled spin qubits in semiconducting QDs that are periodically driven by electrical fields. Inspecting the above expressions, we see that (i) the second term is the analogue of the static spin-photon coupling with the Floquet energy ϵ_q playing the role of the Zeeman splitting E_Z and (ii) the first term, $\propto \Omega$, represents a longitudinal coupling to the resonator and has no analogue for Zeeman-split spin qubits.

Let us first analyse in more details the origins of the qubit splitting. For a Floquet system, the quasi-energy of a state j can be written as $\epsilon_j = \bar{\epsilon}_j - \phi_{G,j}/T$, with^{51,52}

$$\bar{\epsilon}_j = (1/T) \int_0^T dt \langle \psi_j(t) | H_d(t) | \psi_j(t) \rangle, \\ \phi_{G,j} = i \int_0^T dt \langle \psi_j(t) | \partial_t | \psi_j(t) \rangle, \quad (9)$$

being the average energy and the geometrical phase of the Floquet state $|\psi_j(t)\rangle$, respectively. Therefore, in the limit of adiabatic driving, we can identify the quasi-energies as the instantaneous energies $\bar{\epsilon}_{j,\alpha}$ dressed by the adiabatic phases, i. e. $\epsilon_j = \bar{\epsilon}_j - \gamma_{B,j}/T$ with being $\gamma_{B,j} = \gamma_{G,j}(T \rightarrow \infty)$ the corresponding Berry phase. Since for the lowest Kramers doublet $\bar{\epsilon}_0 = \bar{\epsilon}_1$, the entire qubit splitting is generated by the Berry phases in leading order in Ω , $\epsilon_q = \gamma_B \Omega + \mathcal{O}(\Omega^2)$, where $\gamma_B \equiv (\gamma_{0,B} - \gamma_{1,B})/2\pi$ and depends solely on the trajectory of the QDs during the periodic driving. Consequently, the Fourier components of the Floquet qubit photon coupling in Eq. 8 oscillate as

$$g_z(t) \sim k \Omega e^{ik\Omega t}; \quad g_+(t) \sim (\gamma_B + k) \Omega e^{i(\gamma_B + k)\Omega t},$$

with $k = 0, 1, \dots$, allowing to selectively activate them by tuning the resonator frequency close to the corresponding frequencies. For example, when $\omega_c \sim \gamma_B \Omega$, we can disregard the term $\propto g_z(t)$, resulting in a purely transverse coupling like in the static case.⁴³ More interestingly, however, is when $\omega_c \sim \Omega$. Then, switching with the photons to a frame oscillating with Ω , results in the Hamiltonian:

$$H_{s-p} \approx \Delta a^\dagger a + \frac{\Omega}{2} \frac{\mathbf{R}_c}{\lambda_{SO}} \cdot \mathbf{m}_z (k=1) \tau_z^F (a^\dagger + a),$$

where $\Delta = \omega_c - \Omega$, while all the terms that oscillate fast on the time scale $1/\Delta$ have been disregarded. We mention that in a recent work⁵³ it has been proposed a scheme to engineer a longitudinal coupling between Floquet (superconducting) qubits and photons in a microwave resonator. There, for creating such a coupling an additional driving tone was required, on top of the periodic pulse generating the Floquet qubit. Here instead, such longitudinal coupling is induced by the driving itself and, moreover, the separation in frequency (which deactivates the transverse coupling) is caused by the accumulated Berry phase during the cyclic motion. Therefore, such mechanism is intrinsic and does not require additional driving tones, reducing the complexity of the implementation.

A. Specific drivings

To evaluate the Floquet matrix elements in Eq. 8, it is instructive to switch to a frame moving with the QD, which is achieved by the unitary transformation $\mathcal{U}[\mathbf{R}(t)] = e^{i\mathbf{p} \cdot \mathbf{R}(t)}$, so that the isolated QD Hamiltonian becomes:

$$\tilde{H}_d(t) = H_d(0) - \mathbf{p} \cdot \dot{\mathbf{R}}(t), \quad (10)$$

and therefore the entire time-dependence stems from the velocity term $\propto \dot{\mathbf{R}}(t)$. Note that $[\mathcal{U}(\mathbf{R}), \boldsymbol{\sigma}] = 0$, and therefore the spin operator $\boldsymbol{\sigma}$ is the same in the two frames and allows us to use the wave-functions of $\tilde{H}_{el}(t)$ for calculating the matrix elements. Focusing on the adiabatic regime, we can project Eq. 10 onto the lowest degenerate subspace pertaining to $H_{el}(0)$ to obtain the qubit evolution Hamiltonian³⁵ (for more details see Sec. VII):

$$\tilde{H}_s(t) = \frac{1}{\lambda_{SO}} \dot{\mathbf{R}}(t) \cdot \mathbf{m}. \quad (11)$$

Note that this Hamiltonian acts only in the spin space, and therefore the Floquet states will be simply time-dependent superpositions of the basis states $\{| \uparrow \rangle, | \downarrow \rangle\}$:

$$|\psi_1(t)\rangle = \cos\left(\frac{\theta(t)}{2}\right) | \uparrow \rangle + e^{i\phi(t)} \sin\left(\frac{\theta(t)}{2}\right) | \downarrow \rangle, \\ |\psi_0(t)\rangle = e^{-i\phi(t)} \sin\left(\frac{\theta(t)}{2}\right) | \uparrow \rangle - \cos\left(\frac{\theta(t)}{2}\right) | \downarrow \rangle, \quad (12)$$

with the angles $\theta(t)$ and $\phi(t)$ determined by the specific trajectory $\mathbf{R}(t)$. The corrections to these states due to the coupling to the higher orbital levels are $\propto (\Omega/\omega_0)$ and can be neglected in the adiabatic limit. In the following, we discuss two examples of trajectories that lend themselves to exact analytical solutions: (i) linearly and (ii) circularly polarized driving, respectively. To simplify the discussion, in the following we assume only Rashba SOI, which means $\mathbf{m} = (-\sigma_y, \sigma_x, 0)$.

In the case (i), we assume $\mathbf{R}(t) = \mathbf{e}_y R_{0,y} \sin(\Omega t)$, with $R_{0,y}$ the amplitude of the displacement, which gives:

$$H_s(t) = -\frac{\Omega R_{0,y}}{\lambda_{SO}} \sigma_x \cos(\Omega t). \quad (13)$$

The corresponding Floquet quasi-energies and states are $\epsilon_{1,0} = 0$, and⁵⁴

$$|\psi_{0,1}(t)\rangle = \frac{1}{\sqrt{2}} (| \uparrow \rangle \pm | \downarrow \rangle) \sum_{p \in \mathcal{Z}} e^{\pm ip\Omega t} J_p \left(\frac{R_{0,y}}{\lambda_{SO}} \right), \quad (14)$$

where $J_p(x)$ is the Bessel function of second kind. This represents a degenerate Floquet qubit state and therefore any superposition of the above states is also a valid Floquet state. Since these states only posses global time-dependent phases the longitudinal coupling as defined in

Eq. 11 vanishes, $g_z(t) \equiv 0$. However, when $\Omega \sim \omega_c$, we find

$$H_{s-p} \approx \Delta a^\dagger a + 2\Omega \frac{R_{c,x} R_{0,y}}{\lambda_{SO}^2} \tau_x^F (a^\dagger + a), \quad (15)$$

which, up to a π rotation around τ_y^F , is identical to the second term in Eq. 8. That is, when the driving is linear, the spin-photon coupling is purely longitudinal, and can now be utilised for readout, manipulation, and entanglement of remote Floquet spin qubits (see Appendix B for the full general expression). For this coupling to occur, the electric field of the resonator must have a component perpendicular to electrical field inducing the (linear) motion of the QD. Later on, we show that this requirement is related to the crucial role of the non-Abelian Berry curvature associated with the QD motion.

In the case (ii), the dot center performs a circular motion in the SO coupled semiconductor, $\mathbf{R}(t) = R_0(\cos(\Omega t), \sin(\Omega t))$, where R_0 is the radius of the trajectory. When inserted in Eq. 11, it describes a spin 1/2 in a rotating magnetic field, and can be made static by switching to the rotating frame with a transformation $V(t) = \exp(i\Omega\sigma_z t/2)$. This gives:

$$\tilde{H}_s(t) = \frac{\Omega R_0}{\lambda_{SO}} \sigma_x - \frac{\Omega}{2} \sigma_z, \quad (16)$$

and the spectrum

$$E_\pm = \pm \frac{\Omega}{2} \sqrt{1 + \left(\frac{2R_0}{\lambda_{SO}}\right)^2} \equiv \pm \frac{\Omega_R}{2}. \quad (17)$$

Switching back to the original frame, we find the Floquet states as in Eq. 12, with the angle $\theta = \arccos(-\Omega/\Omega_R)$ and $\phi(t) = \Omega t$, while the Floquet qubit splitting is $\epsilon_q = \Omega_R - \Omega$. Using the above wave-functions, we find that when $\Omega \sim \omega_c$ the resulting coupling is longitudinal:

$$H_{s-p} = \Delta a^\dagger a + 2\Omega \frac{R_0 R_c}{\lambda_{SO}^2} (a^\dagger + a) \tau_z^F, \quad (18)$$

where $R_c = \sqrt{R_{c,x}^2 + R_{c,y}^2}$ and we assumed $R_0 \ll \lambda_{SO}$. On the other hand, when the resonator is in resonance with the Floquet qubit, $\omega_c \sim \epsilon_q$:

$$H_{s-p} \approx \Delta a^\dagger a + 2\Omega \frac{R_c}{\lambda_{SO}} \left(\frac{R_0}{\lambda_{SO}}\right)^2 (\tau_+^F a + a^\dagger \tau_-^F), \quad (19)$$

which emulates the well-known Jaynes-Cummings model with all its implications.⁵⁵ Note that R_0 can in principle be arbitrary large, and therefore the only small parameter is R_c/λ_{SO} (while $\Omega \ll \omega_0$ is assumed throughout). For a general trajectory, $\mathbf{R}(t+T) = \mathbf{R}(t)$, the Floquet spectrum and wave-functions can only be evaluated numerically. To test cases that interpolate between the two particular drives discussed above, we have evaluated the spin-photon coupling for elliptic trajectories:

$$\mathbf{R}(t) = (R_{0,x} \cos \Omega t, R_{0,y} \sin \Omega t), \quad (20)$$

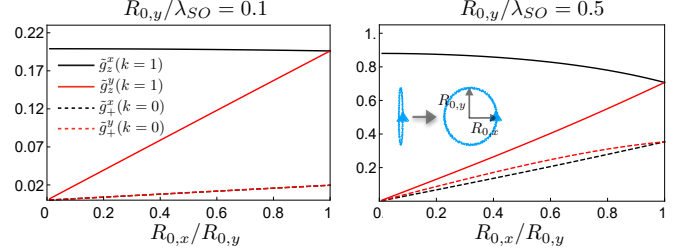


FIG. 2. Variation of the longitudinal, $\tilde{g}_z^{x,y}(k = 1) \equiv m_z^{x,y}(k = 1)$, and transverse $\tilde{g}_+^{x,y}(k = 0) = \gamma_B m_+^{x,y}(k = 0)$ spin-photon coupling strengths with the ellipticity $R_{0,x}/R_{0,y}$ for $R_{0,y}/\lambda_{SO} = 0.1$ (left) and $R_{0,y}/\lambda_{SO} = 0.5$ (right).

where $R_{0,x(y)}$ are the arbitrary amplitudes in the x (y) direction. Indeed, for $R_{0,x} = 0$ ($R_{0,x} = R_{0,y}$) the motion is linear (circular). Specifically, we have calculated numerically the Fourier transforms of the functions $\tilde{g}_z(t) = \dot{\mathbf{m}}_z/\Omega$ and $\tilde{g}_+(t) = (\epsilon_q - d/dt)\mathbf{m}_+/\Omega$ that determine the strength of the spin-photon coupling in Eq. 8. In Fig 2 we show the Fourier components $\tilde{g}_z^{x,y}(k = 1)$ and $\tilde{g}_+^{x,y}(k = 0)$ as a function of $R_{0,x}/R_{0,y}$ for various values of $R_{0,y}/\lambda_{SO}$. Since $\tilde{g}_+^{x,y}(k = 0) \propto \gamma_B$, they both vanish for a linear drive, and increase monotonically towards the circular trajectory where they obey $\tilde{g}_+^x(k = 0) = \tilde{g}_+^y(k = 0)$. Importantly, the longitudinal couplings dominate over the transverse ones in the range $0 \leq R_{0,x}/R_{0,y} \leq 1$, and therefore can be harnessed for various quantum operations.

The strength of the spin-photon coupling is determined by R_c/λ_{SO} , and in order to provide estimates it is instructive to express this ratio as follows:

$$\frac{R_c}{\lambda_{SO}} \equiv \frac{e E_c \lambda_0}{\omega_0} \frac{\lambda_0}{\lambda_{SO}}, \quad (21)$$

and, for simplicity, we fix $R_0/\lambda_{SO} = 0.25$ (which can be achieved by simply changing the driving amplitude depending on the system). We further assume $\Omega = \omega_c/2\pi = 5$ GHz, which represents a typical value for microwave resonators. We focus first on hole spins, which exhibit large SOI, and choose an overall ratio $\lambda_0/\lambda_{SO} = 0.2$. For Ge hole-spin qubits encoded in squeezed dots in Ge/SiGe hetero-structures⁵⁶ (confining length of $\lambda_0 = 50$ nm and $\omega_0/2\pi = 5.2 \times 10^2$ GHz) it means a ratio $R_c/\lambda_{SO} \sim 10^{-3}$, and a coupling strength $g_z \sim 2$ MHz, while for Ge/Si core/shell nanowires ($\lambda_0 = 25$ nm and $\omega_0/2\pi = 9.8$ GHz) QDs we find $R_c/\lambda_{SO} \sim 10^{-2}$ and $g_z \sim 20$ MHz. Also, for Si hole-spin qubits encoded in square fin field-effect transistors (FETs) with $\lambda_0 = 20$ nm and $\omega_0/2\pi = 2 \times 10^2$ GHz,⁵⁶ $R_c/\lambda_{SO} \approx 1.9 \times 10^{-3}$ and $g_z \sim 4$ MHz, for a confinement frequency $\omega_0 \sim 2.4 \times 10^2$ GHz. We note that the SOI can be strongly altered by electrical fields in the case of holes.^{24,48,57,58} For electrons confined in typical GaAs QDs, $\lambda_0 = 50$ nm $\lambda_0/\lambda_{SO} \sim 0.1$, giving $R_c/\lambda_{SO} \approx 5 \times 10^{-5}$ and $g_z \sim 0.1$ MHz. While smaller than in the case of holes, this coupling can be increased by considering cavities with higher frequencies.⁷ For $\omega_c \sim$

50 GHz, the coupling reaches MHz values, comparable to the (transverse) static spin-photon couplings.^{59,60}

IV. FLOQUET SPIN QUBIT READOUT

Both the strength of the Floquet qubit-photon coupling and the Floquet spectrum can be detected from the response of the resonator. The equation of motion for the photon field $a(t)$ for a one-sided resonator coupled to an external line reads:⁶¹

$$\dot{a} = -i\omega_c a + ig_z(t)\tau_z^F - i(g_-(t)\tau_+^F + \text{h.c.}) - \frac{\kappa}{2}a - \sqrt{\kappa}a_{in},$$

where κ is the escape rate of the resonator, a_{in} is the stream of photons impinging on the resonator, and all operators are in the Heisenberg picture. Moreover, the output field exiting the resonator, which is eventually measured, satisfies $a_{out} = a_{in} + \sqrt{\kappa}a$.

A. Longitudinal coupling

Let us first scrutinise the state of the resonator when $\Omega \sim \omega_c$ and the input field is the vacuum. In this case we can retain only the $g_z(t)$ term in the above equation and, more specifically, its $k = \pm 1$ contributions. In the semi-classical regime the average $\alpha(t) = \langle a(t) \rangle$ becomes:⁴⁵

$$\alpha(t) = -i \frac{g_z(k=1)\langle \tau_z^F \rangle}{\kappa} (1 - e^{-\kappa t/2}), \quad (22)$$

resulting in a finite photon population induced by the time-dependent $g_z(t)$. The effect of the qubit on the resonator can be characterised by the measurement pointer state separation $D(t) = |\alpha_+(t) - \alpha_-(t)|$,⁵³ and the signal to noise ratio (SNR):

$$\text{SNR}(t) = \frac{\sqrt{8}|g_z(k=1)|}{\kappa} \sqrt{\kappa t} \left[1 - \frac{2}{\kappa t} (1 - e^{-\kappa t/2}) \right].$$

In the stationary limit $D(\infty) = 2g_z(k=1)/\kappa$ which corresponds to an intra-cavity average photon number $n_{ph} = (2g_z(k=1)/\kappa)^2$. To give some estimates, let us assume a linearly driven QD with an amplitude $R_{0,y}/\lambda_{SO} = 0.25$, so that:

$$n_{ph} \approx \left(Q \frac{eE_c\lambda_0}{\omega_0} \frac{\lambda_0}{\lambda_{SO}} \right)^2, \quad (23)$$

with $Q = \omega_c/\kappa$ being the cavity quality factor. Using the same QD systems discussed in the previous section, and assuming state-of-the art resonators with $Q \sim 10^5$, the average photon number for Ge hole-spin qubits encoded in squeezed dots in Ge/SiGe heterostructures,⁵⁶ $n_{ph} \approx 10^2$, while for Ge/Si core/shell nano wires⁵⁶ $n_{ph} \approx 10^6$. For Si hole-spin qubits encoded in square fin (FETs)⁵⁶ $n_{ph} \approx 10^4$, while for electron spin qubits in gate-defined GaAs QDs $n_{ph} \approx 10^2$. Such photonic populations are easily distinguishable by homodyne detection in current experiments.

B. Transverse coupling

When $\epsilon_q \sim \omega_c$, we can retain in Eq. 22 only the transverse coupling, which pertains to a dispersive readout of the qubit. While this type of measurement is well established,⁶¹ the case of periodic driving has received less attention, and therefore here we give a small account of the approach.^{49,62,63} Let us assume the resonator is driven coherently at the input port with $\epsilon(t) = \epsilon_d \exp(i\omega t)$, with ω being the driving frequency and ϵ_d its amplitude. Then, the input field can be characterised by its mean $\alpha_{in}(t) = \langle a_{in}(t) \rangle = \epsilon(t)/\sqrt{\kappa}$.⁶¹ By treating the term $\propto g_+(t)$ in perturbation theory (see Appendix C for more details on the derivation), the average cavity field obeys the following equation:

$$\dot{\alpha}(t) \approx -i[\omega_c + \chi_\alpha(\omega_c, t)]\alpha(t) - \frac{\kappa}{2}\alpha(t) - \sqrt{\kappa}\alpha_{in}(t),$$

where $\chi_\alpha(\omega_c, t) = \int dt' e^{i\omega_c t'} \chi_\alpha(t', t)$ with:

$$\chi_\alpha(t', t) = -i\theta(t - t') E_{c,\alpha}^2 \langle [r_\alpha^I(t'), r_\alpha^I(t)] \rangle, \quad (24)$$

being the time-dependent susceptibility of the isolated system, and $\langle \dots \rangle$ means the trace over the density matrix of the electrons in the absence of the coupling to photons (here we included the electron-photon couplings into the definition of the susceptibility). In the case of periodic driving the susceptibility obeys $\chi_\alpha(t', t) = \chi_\alpha(t' + T, t + T)$, and can be formally written as:^{62,63}

$$\chi_\alpha(t - \tau, t) = \sum_{q \in \mathcal{Z}} \frac{1}{2\pi} \int d\omega e^{-iq\Omega t - i\omega\tau} \chi_\alpha^q(\omega). \quad (25)$$

Furthermore, in the limit of a good cavity, $\kappa \ll \omega_c, \Omega$, we can retain only the $q = 0$ term in the resulting Fourier transform of Eq. 24 when determining the cavity response. Let us assume the qubit density matrix can be written as $\rho = \sum_\tau \rho_\tau |\psi_\tau(0)\rangle \langle \psi_\tau(0)|$, with ρ_τ being the weight of the Floquet state $\tau = \pm$. This covers the cases when the qubit is in the pure state $\tau = \pm$ (with $\rho_\tau = 1$) and, as demonstrated in the next section, it describes also the stationary state of the qubit in the presence of dissipation. When $\omega \sim \epsilon_q$, we find

$$\chi_\alpha^0(\omega) \approx \epsilon_q^2 \left(\frac{R_{c,\alpha}}{\lambda_{SO}} \right)^2 |m_+^\alpha(k=0)|^2 \frac{\rho_+ - \rho_-}{\omega - \epsilon_q + i\delta},$$

where δ quantifies the line-width of the Floquet levels due to their coupling to the environment. Therefore, the cavity frequency is shifted by a qubit-state dependent term, while the alteration of its Q -factor allows to extract the qubit decoherence rate δ .²² Note that $\epsilon_q \approx \gamma_B \Omega$, and therefore the response vanishes when $\gamma_B \rightarrow 0$, in agreement with the result for a linearly polarised driving. Experimentally, the influence of the qubit on the resonator can be scrutinised from the changes in the resonator transmission as a function of the driving frequency ω of the coherent input state.⁶³

V. DECOHERENCE DUE TO CHARGE FLUCTUATIONS

While the Floquet description allows to determine the spectral feature of the system, it eventually corresponds to an out-of-equilibrium situation. To establish the coherence of the Floquet spin qubit, in the following we evaluate the effects of bosonic baths, such as phonons and charge fluctuations, on its dynamics. We assume the bath couples to the QD as:

$$H_{e-b} = \sum_{\alpha=x,y} e r_{\alpha} \mathcal{E}_{\alpha}, \quad (26)$$

where \mathcal{E}_{α} with $\alpha = x, y$ are the fluctuating electric fields stemming from the environment.^{24,64,65} For $\Omega \ll \omega_0$, the dynamics is restricted to the lowest doublet, and we can project Eq. 26 onto the Floquet qubit subspace. That gives an effective Floquet qubit-bath Hamiltonian $H_{s-b}^I(t) = \sum_{\alpha} e A_{\alpha}(t) \mathcal{E}_{\alpha}(t)$ in the interaction picture, with

$$A_{\alpha}(t) = \sum_{k \in \mathcal{Z}} [r_{\alpha}^z(k) \tau_z^F + r_{\alpha}^+(k) \tau_+^F e^{i\epsilon_q t}] e^{ik\Omega t} + \text{h.c.},$$

where $r_{\alpha}^z(k) = [r_{\alpha}^{11}(k) - r_{\alpha}^{00}(k)]/2$ and $r_{\alpha}^+(k) = r_{\alpha}^{10}(k) = [r_{\alpha}^{01}(-k)]^*$. Let us denote by $\rho(t)$ the reduced density matrix describing the Floquet qubit. That is, $\rho(t) = \text{Tr}_b[\rho_{tot}(t)]$, with $\rho_{tot}(t)$ being the total density matrix of the combined system, and the trace was taken over the bath. Starting from the von-Neumann equation obeyed by the total density matrix, $\dot{\rho}_{tot}(t) = -[H_{tot}(t), \rho_{tot}(t)]$, we can eliminate the bath using the standard approach.⁶⁶ Within the Born approximation, the equation of motion for the reduced density matrix becomes:

$$\frac{d\rho(t)}{dt} = - \int_{-\infty}^t dt' J_{\alpha\beta}(t-t') [A_{\alpha}(t), A_{\beta}(t') \rho(t')] + \text{h.c.} \quad (27)$$

where

$$J_{\alpha\beta}(t-t') = \text{Tr}_B[\mathcal{E}_{\alpha}(t) \mathcal{E}_{\beta}(t') \rho_B] \delta_{\alpha\beta} \equiv J_{\alpha}(t-t'), \quad (28)$$

with the trace taken over the bath degrees of freedom described by the thermal density matrix ρ_B . Its Fourier transform $J_{\alpha}(\omega) = (1/2\pi) \int_{-\infty}^{\infty} dt J_{\alpha}(t) e^{i\omega t}$ it is known as the bath spectral function, and plays a crucial role for describing the dynamics of the qubit.⁶⁷

Substituting $\rho(t') \approx \rho(t)$ on the right hand side of Eq. 27, which amounts to performing also the Markov approximation,⁶⁶ allows us to express the dynamics $\rho(t)$ in a Lindblad form (see Appendix D for details):

$$\dot{\rho}(t) = \sum_{s=\pm,z} \Gamma_s \mathcal{D}_s[\rho(t)], \quad (29)$$

$$\mathcal{D}_s[\rho(t)] = \tau_s \rho(t) \tau_s^{\dagger} - \frac{1}{2} \{ \tau_s^{\dagger} \tau_s, \rho(t) \}, \quad (30)$$

where $\mathcal{D}_s[\rho(t)]$ is the dissipator associated with absorption ($s = +$), emission ($s = -$), and dephasing ($s = z$) processes, respectively, while

$$\begin{aligned} \Gamma_{\pm} &= \left(\frac{\Omega \lambda_0}{\omega_0 \lambda_{SO}} \right)^2 \sum_{\alpha,k} |m_{\pm,\alpha}(k)|^2 (k \pm \gamma_B)^2 J_{\alpha}[\Omega(k \pm \gamma_B)] \\ \Gamma_z &= \left(\frac{\Omega \lambda_0}{\omega_0 \lambda_{SO}} \right)^2 \sum_{\alpha,k} |m_{z,\alpha}(k)|^2 k^2 J_{\alpha}(k\Omega), \end{aligned} \quad (31)$$

are the corresponding rates. Above we neglected a small renormalization of the Floquet spectrum $\propto \Omega^2$ caused by the bosonic bath. While the detailed derivation is presented in the Appendix D, a few comments are in order. To obtain Eq. 30, we have performed the secular approximation, namely we neglected the terms $\propto e^{\pm 2i\epsilon_q t}$ while we retained only the contributions with $q = -k$ in the terms $\propto e^{\pm(k+q)\Omega t}$ in the Eq. 27. This strategy is appropriate if both the minimal quasi-energy difference and the drive frequency Ω are much larger than the inverse of the resulting decoherence rates.⁶⁶ Since in our case $\Gamma_{\pm,z} \propto \Omega^2$, this condition is satisfied automatically in the weak coupling regime, as opposed to periodic drivings by magnetic fields.^{62,66,68} We can identify the relaxation and dephasing times of the Floquet qubit as $1/T_1 = \Gamma_+ + \Gamma_-$ and $1/T_2 = 1/(2T_1) + \Gamma_z$, respectively. Furthermore, the stationary populations of the states $\rho_{\pm} = \Gamma_{\pm}/(\Gamma_+ + \Gamma_-)$ do not obey in general the detailed balance condition $\rho_-/\rho_+ \neq \exp(\Omega/k_B T)$, with T being the temperature. Nevertheless, the density matrix is diagonal in the Floquet basis (in the Schrodinger picture)

$$\rho_S(t) = \sum_{\tau=\pm} \rho_{\tau} |\psi_{\tau}(t)\rangle \langle \psi_{\tau}(t)|, \quad (32)$$

allowing to initialise the Floquet qubit using the dissipation. The above expressions can be contrasted to those describing a static Zeeman-split spin qubit:^{64,65}

$$\Gamma_{\pm}^s = \left(\frac{E_Z \lambda_0}{\omega_0 \lambda_{SO}} \right)^2 \sum_{\alpha=x,y} |m_{+,\alpha}|^2 J_{\alpha}(\pm E_Z), \quad (33)$$

while $\Gamma_z = 0$. We can readily identify Ω as the analogous to E_Z in the expression of the rates and, given the analogy, it means we can infer the decoherence of the Floquet spin qubit from its static counterpart.

To estimate the Floquet spin qubit decoherence times, we need to first specify the spectral function $J_{\alpha}(\omega)$. It is convenient to write it as $J_{\alpha}(\omega) = \rho(\omega) \coth(\frac{\omega}{2T})$ with $\rho(\omega)$ being the spectral density of the bath. For an ohmic bath at low frequencies $\rho(\omega) = \gamma_{\Omega} \omega$, with $\gamma_{\Omega} \sim (e^2/\hbar) \text{Re}[Z]$ being related to the real part of the circuit impedance Z . To give estimates, we assume the same QD parameters as in Sec. III, at $\Omega = \omega_c$, with a bath temperature $T = 40$ mK, and $\gamma_{\Omega} = 10^{-4}$.⁵⁶ In Fig. 3 we show the relaxation rate T_1^{-1} (left), and the pure dephasing rate Γ_z (right) for for Ge hole-spin encoded in squeezed dots, Ge/Si core/shell nanowires QDs,

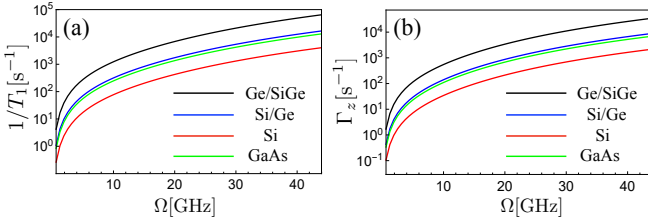


FIG. 3. The relaxation (left) and the pure dephasing (right) rates as function of driving frequency Ω for holes and electrons confined in various semiconducting QDs. We have used $\lambda_0/\lambda_{SO} = 0.2$ for holes (black, red, and blue), while $\lambda_0/\lambda_{SO} = 0.1$ for electrons (green). For all plots we assumed $R_0/\lambda_{SO} = 0.25$, and $T = 40$ mK.

hole spin encoded in square fin Si FETs QDs, and for electron spins in gate-defined GaAs, respectively. We see that these rates stemming from ohmic noises are orders of magnitude smaller than the coupling strengths $|g_{z,+}|$ for all these systems, underlining the robustness of the Floquet spin qubit.

To summarise this section, we identified three features associated with dissipation: (i) the coupling between the environment and the qubit is activated only in the presence of driving, which allows us to perform the secular approximation (ii) the stationary density matrix is diagonal in the Floquet basis (iii) the time-dependent driving induces pure dephasing terms without an analogue in the static Zeeman-split spin qubits.

VI. TWO QUBIT GATES WITH FLOQUET SPIN QUBITS

When two such Floquet qubits are coupled to the same resonator field, the resonator can mediate entangling interactions between the two. Depending on the resonator frequency, such entanglement can be generated by transverse²² or by longitudinal⁴⁶ spin-spin interactions. Here we only discuss the latter mechanism.

Modulating simultaneously the longitudinal coupling between a resonator and qubits allows to implement a high-fidelity controlled-phase gate (CPHASE).^{46,69,70} We show how to implement such a gate for the Floquet qubits where such modulation occurs naturally as a consequence of the Floquet driving itself.

We start by assuming both QDs are driven with the same frequency $\Omega \ll \omega_0$, but can have arbitrary trajectories (therefore different Floquet energies $\epsilon_{q,j}$). Assuming $\Omega \sim \omega_c$, from Eq. 8 we conclude that the minimum requirements for the longitudinal coupling to dominate over the transverse ones in this limit are $|\Omega - \omega_c| \ll |\epsilon_{q,j} - \omega_c|, |\epsilon_{q,j} + \Omega - \omega_c|$, where $\epsilon_{q,j}$ lies within the first Floquet Brillouin zone $-\Omega/2 < \epsilon_{q,j} < \Omega/2$. Interestingly, such a requirement is not present when the QDs are linearly driven as discussed in the previous section. Then, by retaining only the longitudinal terms, we find

the two-qubit Hamiltonian:

$$H_{2q} = \Delta a^\dagger a + (g_{z,1}\tau_{z,1}^F + g_{z,1}\tau_{z,2}^F)(a^\dagger + a), \quad (34)$$

where $\Delta = \omega_c - \Omega$ (the photons are described in a frame rotating with Ω), and $g_{z,j} \equiv g_{z,j}(1)$ are the $k = 1$ components of the longitudinal couplings for the dot $j = 1, 2$. Then, following the exposition in Ref. 47, the evolution operator can be written as:

$$U(t) = e^{i\Delta a^\dagger at} D[\alpha(t)] e^{iJ(t)\tau_{z,1}^F \tau_{z,2}^F}, \quad (35)$$

$$J(t) = \frac{2g_{z,1}g_{z,2}}{\Delta^2} [\Delta t - \sin(\Delta t)], \quad (36)$$

while $D[\alpha(t)] = e^{\alpha(t)a^\dagger - \alpha^*(t)a}$ is a displacement operator that depends on both qubits:

$$\alpha(t) = \frac{1 - e^{i\Delta t}}{\Delta} (g_{z,1}\tau_{z,1}^F + g_{z,2}\tau_{z,2}^F). \quad (37)$$

Modulating the couplings for a time t_g that satisfies $\Delta \cdot t_g = 2n\pi$, with $n = 1, \dots$ and $\frac{2g_{z,1}g_{z,2}}{\Delta} t_g = \pi/4$ decouples the photons from the spins in the dynamics, and implements the entangling CPHASE gate $U_{CP} = \text{diag}[1, 1, 1, -1]$. That in turn is equivalent to choosing the detuning $\Delta = 4\sqrt{ng_{z,1}g_{z,2}}$ and the gate time

$$t_g = \frac{\pi}{2} \sqrt{\frac{n}{g_{z,1}g_{z,2}}} \approx \frac{T}{4} \left(\frac{eE_c\lambda_0}{\omega_0} \frac{\lambda_0}{\lambda_{SO}} \frac{R_0}{\lambda_{SO}} \right)^{-1}, \quad (38)$$

where in the last line, for simplicity, we assumed $g_{z,1} = g_{z,2}$. Therefore, the gate time can be decreased by driving the qubits faster, while the duration of the pulse can be controlled by turning on and off the amplitude of the drive $R_0 \equiv R_0(t)$. Importantly, the CPHASE gate operation as described above remains the same even if the oscillator is initially in a coherent or thermal state, lifting the requirement of any preparation of the oscillator at the start of the gate.^{46,48}

Let us give some estimates for the gate operation time assuming $\Omega = \omega_c = 2\pi \times 5$ GHz, $Q = 10^5$ with all other parameters the same as in Sec. III. For Ge hole-spin qubits encoded in squeezed dots in Ge/SiGe heterostructures, we find $t_g \approx 0.7\mu$ s, for in Ge/Si core/shell nanowires QDs $t_g \approx 6.5$ ns, while for Si hole-spin qubits encoded in square fin (FETs) $t_g \approx 0.1\mu$ s. For electrons in gate-defined GaAs QDs $t_g \approx 1.5\mu$ s, while for InAs QDs encoded in square fin FETs $t_g \approx 4.3\mu$ s.

The fidelity of the CPHASE gate is affected by both photonic loss from the resonator and the intrinsic decoherence mechanisms. The former is independent on the qubit system, and has been discussed at length in Refs. 46 and 47. Therefore, here we only give some estimates based on their findings. The photon-induced dephasing rate is $\Gamma_{ph} \sim 2\kappa \left(\frac{g_z}{2\Delta} \right)^2$, while the gate infidelity scales as⁴⁶

$$1 - \mathcal{F}_{ph} \sim \Gamma_{ph} t_g \approx \left(Q \frac{eE_c\lambda_0}{\omega_0} \frac{\lambda_0}{\lambda_{SO}} \right)^{-1} \sim \frac{1}{\sqrt{n_{ph}}}, \quad (39)$$

where in the last term we assumed, for simplicity, linear driving with $R_{0,y}/\lambda_{SO} = 0.25$ and $n = 1$ (which corresponds to the fastest gate). Therefore, the infidelity due to photon leakage $1 - \mathcal{F}_{ph} \sim 10^{-2} - 10^{-3}$ for the QD systems discussed in the previous section. The above estimates clearly favours the hole-spin implementations: the SOI is strong and it can be manipulated by external electrical fields. We note that the fidelity can be extended, for example, by squeezing the resonator state.⁴⁵ Nevertheless, a full description of the gate operation is beyond the scope of this work and will be left for future studies.

VII. GEOMETRICAL ORIGIN OF THE COUPLING

To elucidate the geometrical underpinnings of Floquet qubit coupled to the resonator, here we utilise the adiabatic perturbation theory to describe the dynamics of a QD in the presence of the microwave resonator in the limit $\Omega \ll \omega_0$. As already anticipated in Sec. V, a unitary transformation $\mathcal{U}[\mathbf{R}(t)] = e^{-i\mathbf{R}(t) \cdot \mathbf{p}}$ on $H_{\text{tot}}(t)$ renders the confining potentials static, at the expense of two novel terms:

$$\tilde{H}_{\text{tot}}(t) = H_{\text{tot}}(0) - \dot{\mathbf{R}} \cdot \mathbf{p} - e\mathbf{E}_c \cdot \mathbf{R}(a^\dagger + a). \quad (40)$$

The second term ($\propto \dot{\mathbf{R}}$) quantifies a Galilean boost associated with uniform translations, while the third ($\propto \mathbf{R}$) represents a time-dependent displacement in the photonic field. However, it is easy to check that the latter does not affect the dynamics in leading order in the velocity $\dot{\mathbf{R}}$ and can be disregarded (it can be gauged away in leading order). In the absence of the resonator, external magnetic and electric fields, each electron or hole QD displays a spectrum of degenerate Kramers doublets, as discussed in Sec. III.

We start by treating the term $\propto \mathbf{R}(t)$ in perturbation theory with respect to the static (and decoupled from the photons) QD Hamiltonian $H_d(0)$. That is, we perform a (time-dependent) Schrieffer-Wolff transformation of the total Hamiltonian, $\mathcal{U}(t) = e^S = 1 + S + S^2/2 + \dots$, such that $[S, H_d(0)] + (1 - \mathcal{P}_0) \dot{\mathbf{R}} \cdot \mathbf{p} = 0$, where \mathcal{P}_0 is a projector onto the lowest degenerate subspace. Reinstating the electron-photon coupling, the resulting Hamiltonian becomes

$$H_{s-p}(t) = \frac{\dot{R}_\alpha}{\lambda_{SO}} \left(\mathcal{A}_\alpha - \frac{R_{c,\beta}}{\lambda_{SO}} \mathcal{F}_{\alpha\beta}(a^\dagger + a) \right) + \omega_c a^\dagger a,$$

where $\mathcal{A}_\alpha \equiv \mathcal{P}_0 p_\alpha \mathcal{P}_0 = m_\alpha$ and $\mathcal{F}_{\alpha\beta} = i[\mathcal{A}_\alpha, \mathcal{A}_\beta] = 2\sigma_z \epsilon_{\alpha\beta z} / \lambda_{SO}^2$ with $\alpha = x, y$ and $\epsilon_{\alpha\beta\gamma}$ the Levi-Civita symbol, are the non-Abelian Berry connection and curvature, respectively, associated with the electron or hole spin confined in the SO coupled QD.⁷⁵ Since $S \propto \dot{\mathbf{R}}$, the terms neglected are $\propto (\dot{\mathbf{R}})^2, \ddot{\mathbf{R}}$. Therefore, in this description, the isolated dynamics is dictated by the Berry

connection, while the coupling to the resonator is mediated by the non-Abelian Berry curvature.⁷⁵ When the driving is periodic, $\mathbf{R}(t+T) = \mathbf{R}(t)$, it is straightforward to show that the above Hamiltonian reproduces both the linearly polarised (Eq. 15) and circularly polarised drive (Eqs. (18),(19)) results.

The adiabatic framework allows us to extend to cases when the QD confinement is arbitrary, not only harmonic. Then, the time-dependent electric field $\mathbf{E}(t+T) = \mathbf{E}(t)$ does not only shift the center of the QD, but also modifies its shape. In this case, following Ref. 75, we use a unitary transformation $\mathcal{U} \equiv \mathcal{U}[\mathbf{E}(t)]$ which diagonalises the Hamiltonian in the instantaneous basis including the drive, $H_d(t)$, to find:

$$H_{s-p}(t) = \dot{E}_\alpha [\mathcal{A}_\alpha^E + E_{c,\beta} \mathcal{F}_{\alpha\beta}^E(a^\dagger + a)] + \omega_c a^\dagger a, \quad (41)$$

where now $\mathcal{A}_\alpha^E = i\mathcal{U}^\dagger \partial_{E_\alpha} \mathcal{U}$ and $\mathcal{F}_{\alpha\beta}^E = \partial_\alpha \mathcal{A}_\beta^E - \partial_\beta \mathcal{A}_\alpha^E + i[\mathcal{A}_\alpha^E, \mathcal{A}_\beta^E]$ are, respectively, the Berry connection and curvature pertaining to the changes in the applied electrical field. Then, the evolution operator is determined by $H_s^0(t) = \dot{E}_\alpha \mathcal{A}_\alpha^E$, which can be formally written in the same form as in Eq. 6, with $j = 0, 1$. Finally, the spin-photon coupling in the interaction picture becomes:

$$H_{s-p} = E_{c,\beta} \left(m_\beta^z \tau_z^F + m_\beta^+ e^{i\epsilon_q t} \tau_+^F + \text{h.c.} \right) (a^\dagger + a),$$

where $m_\beta^z(t) = \dot{E}_\alpha (\langle \psi_1(t) | \mathcal{F}_{\alpha\beta}^E | \psi_1(t) \rangle - \langle \psi_0(t) | \mathcal{F}_{\alpha\beta}^E | \psi_0(t) \rangle)$ and $m_\beta^+(t) = \dot{E}_\alpha \langle \psi_0(t) | \mathcal{F}_{\alpha\beta}^E | \psi_1(t) \rangle = [m_{\alpha\beta}^-(t)]^*$ are periodic functions $\propto \Omega$ (because of \dot{E}_α), and $\epsilon_q \propto \Omega$ is the quasi-energy. Therefore, in perfect analogy with the harmonic confinement, by tuning the cavity in resonance with Ω (ϵ_q) it is possible to activate the term $\propto \tau_z^F$ ($\propto \tau_+^F$) which corresponds to a longitudinal (transverse) spin-photon coupling.

VIII. CONCLUSIONS AND OUTLOOK

In this work, we studied the interaction between spins (electron or hole) in QDs that are periodically driven by electrical fields, and the photons in a microwave resonator. Using the Floquet theory, we showed that the spin-orbit interactions induces a time-dependent magnetic field that acts within the ground state Kramer's doublets, and generates spin-photons interactions in the absence of any applied magnetic fields. We found both transverse and longitudinal coupling of the Floquet qubit to the resonator, with the latter being a novel contribution having no analogue for static Zeeman-split spin qubits. We demonstrated that such longitudinal interactions facilitate both the readout of the qubit, and the implementation of a CPHASE gate in the case of two remote QDs coupled to the same cavity. Finally, using an adiabatic perturbation theory, we have uncovered the geometrical origin of these dynamical effects and demonstrated their generality to arbitrary QD confinements.

System	$\omega_0/2\pi$ [GHz]	E_c [Vm $^{-1}$]	R_c/l_{SO}	$g_z/(2\pi)$ [MHz]	n_{ph}	t_g [ns]
Hole-spins in Ge/SiGe heterostructures ⁷¹	10^2	1.6×10^2	4×10^{-3}	10	10^5	50
Hole-spins in Ge/Si core/shell NW ⁷²	4×10^2	3.2×10^2	10^{-3}	2.4	10^4	200
Hole-spins in Si square fin FET ⁷³	2×10^2	4×10^2	2×10^{-2}	5	10^5	100
Electron-spins in GaAs 2DEG ⁷⁴	1.1×10^2	1.6×10^2	1.8×10^{-3}	4	10^5	100

TABLE I. Estimates for the longitudinal spin-photon coupling (g_z), average number of photons in the resonator (n_{ph}), and two-qubit CPHASE gate time (t_g) for various semiconducting QDs. We assumed $\lambda_0/\lambda_{SO} = 0.2$ ($\lambda_0/\lambda_{SO} = 0.1$) for holes (electrons). The cavity frequency is $\omega_c = \Omega = 2\pi \times 5$ GHz with a quality factor $Q = 10^5$. For all systems we assumed $R_0/\lambda_{SO} = 0.25$.

A summary of our results is presented in Table I, for both hole and electron spins in semiconducting nanostructures.

There are several possible future directions. First, it is straightforward to generalise to more driven spin qubits because the QDs do not interact directly with each other. A more non-trivial extension, in particular for hole-spins in QDs, is to determine microscopically the effect of the electrical fields on both the SOI and the dynamics.²⁴ Furthermore, it would be beneficial to evaluate the phonon-induced decoherence for the driven hole-spin qubits for more realistic confining potentials and identify sweet spots for their operation. Further down the road, it would be interesting to extract the statistics of the electromagnetic field emitted because of the driving and establish the imprints of the spin-qubit geometry

of states onto the photons.^{55,76}

In conclusion, the Floquet qubit proposed in this work operates well within the current experimental capabilities and we expect it to open up new possibilities for future studies on driven spin qubits in the absence of externally applied magnetic fields.

ACKNOWLEDGMENTS

This work was supported by the Foundation for Polish Science through the International Research Agendas (IRA) program co-financed by the European Union within Smart Growth Programme, and by the National Science Centre (Poland) OPUS 2021/41/B/ST3/04475.

Appendix A: Identities valid for parabolic QD confinement

When the confinement of the QDs is harmonic, we can establish relationships between various matrix elements (setting $\hbar = 1$):³⁵

$$\langle \psi_j | [\mathbf{p}, H_{el}] | \psi_{j'} \rangle = (\epsilon_{j'} - \epsilon_j) \langle \psi_j | \mathbf{p} | \psi_{j'} \rangle \equiv -im\omega_0^2 \langle \psi_j | \mathbf{r} | \psi_{j'} \rangle \quad (42)$$

and

$$\langle \psi_j | [\mathbf{r}, H_{el}] | \psi_{j'} \rangle = (\epsilon_{j'} - \epsilon_j) \langle \psi_j | \mathbf{r} | \psi_{j'} \rangle \equiv \frac{i}{m} \langle \psi_j | \mathbf{P} | \psi_{j'} \rangle, \quad (43)$$

where $\mathbf{P} = \mathbf{p} + \mathbf{m}/\lambda_{SO}$ and $\mathbf{m} = \lambda_{SO} \lambda_{SO}^{-1} \boldsymbol{\sigma}$, with $\|\lambda_{SO}^{-1}\| = m\sqrt{\alpha^2 + \beta^2}$. That in turn implies

$$-\langle \psi_j | \mathbf{p} | \psi_{j'} \rangle = \frac{1}{\lambda_{SO}} \frac{\omega_0^2}{\omega_0^2 - (\epsilon_j - \epsilon_{j'})^2} \langle \psi_{j'} | \mathbf{m} | \psi_{j'} \rangle, \quad (44)$$

$$-\langle \psi_j | \mathbf{r} | \psi_{j'} \rangle = -\frac{i}{m\lambda_{SO}} \frac{\epsilon_j - \epsilon_{j'}}{\omega_0^2 - (\epsilon_j - \epsilon_{j'})^2} \langle \psi_j | \mathbf{m} | \psi_{j'} \rangle. \quad (45)$$

Hence, the momentum and position operators, respectively, projected onto the two lowest states $\{|\psi_0\rangle, |\psi_1\rangle\}$ become:

$$\tilde{\mathbf{p}} \equiv \mathcal{P}_0 \mathbf{p} \mathcal{P}_0 = \frac{1}{\lambda_{SO}} \left(\frac{\omega_0^2}{\omega_0^2 - \epsilon_q^2} (\mathbf{m}_+ \tau_+ + \mathbf{m}_- \tau_-) + \frac{1}{2} \mathbf{m}_z \tau_z \right), \quad (46)$$

$$\tilde{\mathbf{r}} = \mathcal{P}_0 \mathbf{r} \mathcal{P}_0 = \frac{i}{m\lambda_{SO}} \frac{\epsilon_q}{\omega_0^2 - \epsilon_q^2} (\mathbf{m}_+ \tau_+ - \mathbf{m}_- \tau_-), \quad (47)$$

where $\epsilon_q = \epsilon_1 - \epsilon_0$ and

$$\mathbf{m}_+ = (\mathbf{m}_-)^* = \langle \psi_1 | \mathbf{m} | \psi_0 \rangle, \quad (48)$$

$$\mathbf{m}_z = \langle \psi_1 | \mathbf{m} | \psi_1 \rangle - \langle \psi_0 | \mathbf{m} | \psi_0 \rangle, \quad (49)$$

$$\frac{1}{\lambda_{SO}} = \frac{1}{\sqrt{2}} \|\boldsymbol{\lambda}_{SO}^{-1}\|. \quad (50)$$

In the above expressions, $\boldsymbol{\tau} = (\tau_x, \tau_y, \tau_z)$ are Pauli matrices acting on the subspace defined by the pair $\{|\psi_0\rangle, |\psi_1\rangle\}$. These expressions are valid in the absence of the coupling to the photons and apply also when an external magnetic field is present. Therefore, the electron-photon Hamiltonian acting in the doublet subspace reads:

$$H_{s-p} = \mathcal{P}_0 H_{e-p} \mathcal{P}_0 = i \frac{e}{m \lambda_{SO}} \frac{E_Z}{\omega_0^2 - \epsilon_q^2} \mathbf{E}_c \cdot (\mathbf{m}_+ \tau_+ - \mathbf{m}_- \tau_-) (a^\dagger + a) \approx i E_Z \frac{\mathbf{R}_c}{\lambda_{SO}} \cdot (\mathbf{m}_+ \tau_+ - \mathbf{m}_- \tau_-) (a^\dagger + a), \quad (51)$$

where in the last line we assumed $E_Z \ll \omega_0$ and defined $\mathbf{R}_c = \frac{e}{m} \frac{\mathbf{E}_c}{\omega_0^2}$ as the distance the cavity field electrical field shifts the center of the QD. This constitutes the expression depicted in the main text.

The above relationships can be extended to the periodically driven case. Starting from the matrix element of an operator \mathcal{O} of the system in the interaction picture becomes:

$$\mathcal{O}^I(t) = \sum_{j,j'} \langle \psi_j(t) | \mathcal{O} | \psi_{j'}(t) \rangle | \psi_j(0) \rangle \langle \psi_{j'}(0) | e^{i(\epsilon_j - \epsilon_{j'})t}, \quad (52)$$

which contain both the two Floquet qubit states stemming from the originally degenerate Kramers doublet, as well as the higher ones. Moreover:

$$\langle \psi_j(t) | \mathcal{O} | \psi_{j'}(t) \rangle = \sum_k e^{ik\Omega t} \mathcal{O}_{jj'}(k), \quad (53)$$

$$\mathcal{O}_{jj'}(k) = \frac{1}{T} \int_0^T dt e^{-ik\Omega t} \langle \psi_j(t) | \mathcal{O} | \psi_{j'}(t) \rangle. \quad (54)$$

Therefore, in the Fourier space we obtain the following identities:

$$(\epsilon_j - \epsilon_{j'} + k\Omega) \mathbf{p}_{jj'}(k) = -im\omega_0^2 \mathbf{r}_{jj'}(k), \quad (55)$$

$$(\epsilon_j - \epsilon_{j'} + k\Omega) \mathbf{r}_{jj'}(k) = \frac{i}{m} \mathbf{P}_{jj'}(k), \quad (56)$$

Finally, the analogous of the static relations become:

$$\mathbf{p}_{jj'}(k) = -\frac{1}{\lambda_{SO}} \frac{\omega_0^2}{\omega_0^2 - (\epsilon_j - \epsilon_{j'} + k\Omega)^2} \mathbf{m}_{jj'}(k), \quad (57)$$

$$\mathbf{r}_{jj'}(k) = \frac{i}{m\lambda_{SO}} \frac{\epsilon_j - \epsilon_{j'} + k\Omega}{\omega_0^2 - (\epsilon_j - \epsilon_{j'} + k\Omega)^2} \mathbf{m}_{jj'}(k), \quad (58)$$

where $\mathbf{m}_{jj'}(k)$ is the k -th Fourier component of $\langle \psi_j(t) | \mathbf{m} | \psi_{j'}(t) \rangle$. These identities can be utilised to express the electron-photon Hamiltonian in the Floquet basis in the interaction picture:

$$H_{e-p}^I(t) = i \frac{e}{m \lambda_{SO}} \sum_{j,j'} \sum_k e^{i(\epsilon_j - \epsilon_{j'} + k\Omega)t} \frac{\epsilon_j - \epsilon_{j'} + k\Omega}{\omega_0^2 - (\epsilon_j - \epsilon_{j'} + k\Omega)^2} \mathbf{E}_c \cdot \mathbf{m}_{jj'}(k) | \psi_j(0) \rangle \langle \psi_{j'}(0) | (a^\dagger e^{i\omega_c t} + a e^{-i\omega_c t}). \quad (59)$$

We can further simplify this expression when the driving is adiabatic, that is when

$$\Omega \ll \min |\bar{\epsilon}_j - \bar{\epsilon}_{j'}|, \quad (60)$$

when the levels j and j' do not belong to the same Kramers doublet in the absence of driving. We therefore define:

$$\begin{aligned} \tau_x^F &= |\psi_0(0)\rangle \langle \psi_1(0)| + |\psi_1(0)\rangle \langle \psi_0(0)|, \\ \tau_y^F &= i(|\psi_0(0)\rangle \langle \psi_1(0)| - |\psi_1(0)\rangle \langle \psi_0(0)|), \\ \tau_z^F &= |\psi_1(0)\rangle \langle \psi_1(0)| - |\psi_0(0)\rangle \langle \psi_0(0)|. \end{aligned} \quad (61)$$

This constitutes the dynamical analogue of the static Zeeman-split spin qubit case. Projecting the interaction Hamiltonian onto this subspace we find:

$$\begin{aligned}
H_{s-p}^I(t) &\approx \frac{ie\Omega}{m\omega_0^2} \sum_k ke^{ik\Omega t} \mathbf{E}_c \cdot [\mathbf{m}_{11}(k) - \mathbf{m}_{00}(k)] \frac{\tau_z^F}{2} (a^\dagger e^{i\omega_c t} + \text{h.c.}) \\
&+ \frac{ie}{m\omega_0^2} \sum_k (\epsilon_q + k\Omega) \mathbf{E}_c \cdot \left[e^{i(\epsilon_q + k\Omega)t} \mathbf{m}_{10}(k) \tau_+^F - e^{-i(\epsilon_q + k\Omega)t} \mathbf{m}_{01}(-k) \tau_-^F \right] (a^\dagger e^{i\omega_c t} + \text{h.c.}) \\
&= \left(\underbrace{\frac{\mathbf{R}_c}{2\lambda_{SO}} \cdot \frac{d}{dt} \mathbf{m}_z(t) \tau_z^F}_{g_z(t)} + \underbrace{i \frac{\mathbf{R}_c}{\lambda_{SO}} \cdot e^{i\epsilon_q t} \left(\epsilon_q - i \frac{d}{dt} \right) \mathbf{m}_+(t) \tau_+^F}_{g_+(t)} + \text{h.c.} \right) (a^\dagger e^{i\omega_c t} + \text{h.c.}),
\end{aligned} \tag{62}$$

where $\epsilon_q = \epsilon_1 - \epsilon_0$, while we defined $\mathbf{m}_+(t) = \langle \psi_1(t) | \mathbf{m} | \psi_0(t) \rangle = [\mathbf{m}_-(t)]^*$ and $\mathbf{m}_z(t) = \langle \psi_1(t) | \mathbf{m} | \psi_1(t) \rangle - \langle \psi_0(t) | \mathbf{m} | \psi_0(t) \rangle$.

Appendix B: Linearly polarised electrical driving

Here we give more details for the case when the QD is driven linearly. Specifically, we assume:

$$\mathbf{R}(t) = \mathbf{e}_y R_{0,y} \sin(\Omega t). \tag{63}$$

It is instructive to switch to the moving frame, which is achieved by a transformation $\mathcal{U}[\mathbf{R}(t)] = e^{i\mathbf{p} \cdot \mathbf{R}(t)}$, leading to the lowest doublet Hamiltonian:

$$H_s(t) = \frac{\dot{\mathbf{R}}(t)}{\lambda_{SO}} \cdot \mathbf{m}, \tag{64}$$

where we only kept the lowest order effects in the SOI (otherwise, $\lambda_{SO}^{-1} \boldsymbol{\sigma}$ needs to be substituted by $\mathcal{P}_0 \lambda_{SO}^{-1} \boldsymbol{\sigma} \mathcal{P}_0$). To simplify the discussion, we assume only Rashba SOI. In this case, we can further write:

$$H_s(t) = -\frac{\Omega R_{0,y}}{\lambda_{SO}} \sigma_x \cos(\Omega t). \tag{65}$$

The corresponding Floquet quasi-energies and states are $\epsilon_{1,0} = 0$

$$|0, 1(t)\rangle = \frac{1}{\sqrt{2}} (|\uparrow\rangle \pm |\downarrow\rangle) e^{\pm i \frac{R_{0,y} \sin(\Omega t)}{\lambda_{SO}}} = \frac{1}{\sqrt{2}} (|\uparrow\rangle \pm |\downarrow\rangle) \sum_{p \in \mathcal{Z}} e^{\pm i p \Omega t} J_p(R_{0,y}/\lambda_{SO}), \tag{66}$$

where $J_p(x)$ is the Bessel function of second kind. Since these states only posses global phases $g_z(t) \equiv 0$, while for the second term generates the whole spin-photon Hamiltonian:

$$H_{s-p}(t) = 2\Omega \frac{R_{c,x} R_{0,y}}{\lambda_{SO}^2} \cos(\Omega t) e^{\pm 2i \frac{R_{0,y} \sin(\Omega t)}{\lambda_{SO}}} \tau_+^F (a^\dagger e^{i\omega_c t} + a e^{-i\omega_c t}) + \text{h.c.}, \tag{67}$$

where $R_{c,x} = eE_{c,x}/m\omega_0^2$ quantifies the displacement of the QD by the cavity electric field. Assuming the driving frequency is tuned close to the cavity frequency, $\Omega \sim \omega_c$, we can retain in the above expression only the terms that oscillate slowly on their respective scale. These terms read:

$$H_{s-p} \approx 2\Omega \frac{R_{c,x} R_{0,y}}{\lambda_{SO}^2} \tau_x^F (a^\dagger + a), \tag{68}$$

as depicted in Eq. 15 in the main text.

Appendix C: Details on the input-output approach for detection

Starting from the equation of motion for the photon field reads:

$$\dot{a}(t) = -i\omega_c a(t) + ieE_{c,\alpha}r_\alpha(t) - \frac{\kappa}{2}a(t) - \sqrt{\kappa}a_{in}(t), \quad (69)$$

where $r_\alpha(t)$ is the position operator in the Heisenberg picture, we can express it in leading order in the coupling to the photons as:

$$r_\alpha(t) \approx r_\alpha^I(t) + ieE_{c,\alpha} \int_{-\infty}^t d\tau (a^\dagger + a)(\tau) [r_\alpha^I(\tau), r_\alpha^I(t)]. \quad (70)$$

Let us assume the cavity is driven continuously with $\epsilon(t) = \epsilon_d \exp(i\omega_d t)$, with ω_d being the driving frequency. Then, the input field can be characterised by its mean $\alpha_{in}(t) = \langle a_{in}(t) \rangle$, where $\alpha_{in}(t) = \epsilon(t)/\sqrt{\kappa}$. Fluctuations around the input value will determine the noise magnitude in the detection signal. On top of that, the following relation holds between the input, output, and the cavity field:

$$a_{out}(t) = a_{in}(t) + \sqrt{\kappa}a(t), \quad (71)$$

which also holds for the averages $\alpha_{out}(t) = \alpha_{in}(t) + \sqrt{\kappa}\alpha(t)$. Then, the average cavity field obeys the following equation:

$$\dot{\alpha}(t) \approx -i\omega_c \alpha(t) + iE_{c,\alpha} \langle r_\alpha^I(t) \rangle - i\alpha(t) \int_{-\infty}^{\infty} d\tau e^{-i\omega_c \tau} \chi_\alpha(t - \tau, t) - \frac{\kappa}{2}\alpha(t) - \sqrt{\kappa}\alpha_{in}(t), \quad (72)$$

where

$$\chi_\alpha(t', t) = -i\theta(t - t') E_{c,\alpha}^2 \langle [r_\alpha^I(t'), r_\alpha^I(t)] \rangle, \quad (73)$$

is the time-dependent susceptibility of the isolated system, and $\langle \dots \rangle$ means the trace over the stationary density matrix of the electrons in the absence of the coupling to photons (here we included the couplings into the definition). In the case of periodic driving and in the stationary regime, the susceptibility obeys $\chi_\alpha(t', t) = \chi_\alpha(t' + T, t + T)$, and can be formally written as:

$$\chi_\alpha(t - \tau, t) = \sum_k \frac{1}{2\pi} \int d\omega e^{-ik\Omega t - i\omega\tau} \chi_\alpha^k(\omega), \quad (74)$$

which in turn allows to write the Fourier transformed equation of motion:

$$-i\omega\alpha(\omega) = -i\omega_c \alpha(\omega) + \sum_q \chi_\alpha^q(\omega) \alpha(\omega - q\Omega) - \frac{\kappa}{2}\alpha(\omega) + iE_{c,\alpha} \langle r_\alpha^I(\omega) \rangle - \sqrt{\kappa}\alpha_{in}(\omega). \quad (75)$$

Assuming the density matrix can is $\rho = \sum_\tau \rho_\tau^F |\psi_\tau(0)\rangle\langle\psi_\tau(0)|$, with ρ_τ^F being the weight of the Floquet state $\tau = \pm$, we find for the $q = 0$ Fourier component:

$$\begin{aligned} \chi_\alpha^0(\omega) &= E_{c,\alpha}^2 \sum_{\tau,\tau'} \sum_k \rho_\tau^F \left[\frac{r_{\tau\tau'}^\alpha(-k) r_{\tau'\tau}^\alpha(k)}{\omega + \epsilon_\tau - \epsilon_{\tau'} + k\Omega + i\delta} - \frac{r_{\tau\tau'}^\alpha(k) r_{\tau'\tau}^\alpha(-k)}{\omega - \epsilon_\tau + \epsilon_{\tau'} + k\Omega + i\delta} \right] \\ &= E_{c,\alpha}^2 \sum_\tau \sum_k (\rho_\tau^F - \rho_{\bar{\tau}}^F) \frac{r_{\tau\bar{\tau}}^\alpha(-k) r_{\bar{\tau}\tau}^\alpha(k)}{\omega + \epsilon_\tau - \epsilon_{\bar{\tau}} + k\Omega + i\delta} \\ &= \frac{E_{c,\alpha}^2}{(\hbar m \omega_0^2)^2} \sum_\tau \sum_k (\rho_\tau^F - \rho_{\bar{\tau}}^F) \frac{(\epsilon_\tau - \epsilon_{\bar{\tau}} + k\Omega)^2}{\omega + \epsilon_\tau - \epsilon_{\bar{\tau}} + k\Omega + i\delta} \mathcal{M}_{\tau\bar{\tau}}^\alpha(-k) \mathcal{M}_{\bar{\tau}\tau}^\alpha(k), \end{aligned} \quad (76)$$

where δ quantifies the linewidth of the Floquet levels (assumed to be the same for all levels, for simplicity).

Let us evaluate the response when the QD is driven on a circular trajectory. Then, using the Floquet states in Eq. 12 in the main text, we find

$$\sigma_{01,y}(k) = \frac{i}{T} \int_0^T dt e^{-ik\Omega t} [e^{2i\Omega t} \sin^2(\theta/2) + \cos^2(\theta/2)] = i[\sin^2(\theta/2) \delta_{k,2} + \cos^2(\theta/2) \delta_{k0}] = [\sigma_{10,y}(-k)]^*, \quad (77)$$

$$\sigma_{01,x}(k) = \frac{1}{T} \int_0^T dt e^{-ik\Omega t} [e^{2i\Omega t} \sin^2(\theta/2) - \cos^2(\theta/2)] = [\sin^2(\theta/2) \delta_{k,2} - \cos^2(\theta/2) \delta_{k0}] = [\sigma_{10,x}(-k)]^*, \quad (78)$$

which can be substituted in the expression for the susceptibility to give

$$\begin{aligned}
\chi_\alpha^0(\omega) &= \left(\frac{R_{c,\alpha}}{\lambda_{SO}}\right)^2 \sum_\tau \sum_k (\rho_\tau^F - \rho_{\bar{\tau}}^F) \frac{(\epsilon_\tau - \epsilon_{\bar{\tau}} + k\Omega)^2}{\omega + \epsilon_\tau - \epsilon_{\bar{\tau}} + k\Omega + i\delta} [\sin^4(\theta/2)\delta_{k,-2} + \cos^4(\theta/2)\delta_{k,0}] \\
&= \left(\frac{R_{c,\alpha}}{\lambda_{SO}}\right)^2 \sum_\tau (\rho_\tau^F - \rho_{\bar{\tau}}^F) \left[\frac{(\epsilon_\tau - \epsilon_{\bar{\tau}} - 2\Omega)^2}{\omega + \epsilon_\tau - \epsilon_{\bar{\tau}} - 2\Omega + i\delta} \sin^4(\theta/2) + \frac{(\epsilon_\tau - \epsilon_{\bar{\tau}})^2}{\omega + \epsilon_\tau - \epsilon_{\bar{\tau}} + i\delta} \cos^4(\theta/2) \right] \\
&\approx \frac{(\Omega\gamma_B)^2}{4(\gamma_B + 1)^2} \left(\frac{R_{c,\alpha}}{\lambda_{SO}}\right)^2 (\rho_+^F - \rho_-^F) \left[\frac{(\gamma_B - 2)^2}{\omega + (\gamma_B - 2)\Omega + i\delta} - \frac{(\gamma_B + 2)^2}{\omega - (\gamma_B + 2)\Omega + i\delta} + \frac{(\gamma_B + 2)^2}{\omega - \gamma_B\Omega + i\delta} \right]. \quad (79)
\end{aligned}$$

We see that when $\omega \sim \gamma_B\Omega$, this simplifies to the result obtained in the main text, while the response vanishes when $\gamma_B \rightarrow 0$, in accordance with the result for the linearly polarised driving.

Appendix D: Floquet-Born-Markov approach to dissipation

Assuming that the relevant dynamics occurs within the originally degenerate subspace, the Floquet qubit-bath interaction Hamiltonian reads (in the interaction picture):

$$H_{s-b}^I(t) = \sum_{\alpha,k} \underbrace{e [r_\alpha^z(k)\tau_z^F + r_\alpha^+(k)\tau_+^F e^{-i\epsilon_q t} + r_\alpha^-(k)\tau_-^F e^{i\epsilon_q t}]}_{A_\alpha(t)} e^{ik\Omega t} \mathcal{E}_\alpha(t),$$

where we only retained the terms that do not act as identity in this subspace. In this case, we assume the entire population of the QD is localized in this subspace, and therefore describe the evolution of the Floquet qubit by its density matrix (in the Born approximation):

$$\frac{d\rho(t)}{dt} = - \int_{t_0}^t dt' \text{Tr}_B \{ H_{s-b}^I(t), [H_{s-b}^I(t'), \rho(t) \otimes \rho_B] \} = - \int_{t_0}^t dt' J_{\alpha\beta}(t-t') [A_\alpha(t), A_\beta(t') \rho(t')] + \text{h.c.} \quad (80)$$

where

$$J_{\alpha\beta}(t-t') = \text{Tr}_B [\mathcal{E}_\alpha(t) \mathcal{E}_\beta(t') \rho_B] \delta_{\alpha\beta} \equiv J_\alpha(t-t'), \quad (81)$$

being the bath correlation function and ρ_B is the density matrix of the bath (for simplicity, we have assumed the cross correlations between different components vanish). Utilising also the Markov approximation, which means on the right hand side we can take $\rho(t') \approx \rho(t)$, allows us to determine the evolution of the density matrix as follows:

$$\begin{aligned}
\frac{d\rho(t)}{dt} &= - \int_{-\infty}^{\infty} d\omega \int_{-\infty}^t dt' \sum_\alpha J_\alpha(\omega) e^{i\omega(t-t')} \sum_{k,q} e^{ik\Omega t} e^{iq\Omega t'} \\
&\quad \times \left[(r_\alpha^z(k)\tau_z^F + r_\alpha^+(k)\tau_+^F e^{i\epsilon_q t} + r_\alpha^-(k)\tau_-^F e^{-i\epsilon_q t})(r_\alpha^z(q)\tau_z^F + r_\alpha^+(q)\tau_+^F e^{i\epsilon_q t'} + r_\alpha^-(q)\tau_-^F e^{-i\epsilon_q t'}) \rho(t) \right. \\
&\quad \left. - (r_\alpha^z(q)\tau_z^F + r_\alpha^+(q)\tau_+^F e^{i\epsilon_q t'} + r_\alpha^-(q)\tau_-^F e^{-i\epsilon_q t'}) \rho(t) (r_\alpha^z(k)\tau_z^F + r_\alpha^+(k)\tau_+^F e^{i\epsilon_q t} + r_\alpha^-(k)\tau_-^F e^{-i\epsilon_q t'}) \right] + \text{h.c.} \quad (82) \\
&= -i \int_{-\infty}^{\infty} d\omega \sum_\alpha J_\alpha(\omega) \sum_{k,q} e^{i(k+q)\Omega t} \\
&\quad \times \left[(r_\alpha^z(k)\tau_z^F + r_\alpha^+(k)\tau_+^F e^{i\epsilon_q t} + r_\alpha^-(k)\tau_-^F e^{-i\epsilon_q t}) \left(\frac{r_\alpha^z(q)}{\omega - q\Omega + i\eta} \tau_z^F + \frac{r_\alpha^+(q)e^{i\epsilon_q t}}{\omega - \epsilon_q - q\Omega + i\eta} \tau_+^F + \frac{r_\alpha^-(q)e^{-i\epsilon_q t}}{\omega + \epsilon_q - q\Omega + i\eta} \tau_-^F \right) \rho(t) \right. \\
&\quad \left. - \left(\frac{r_\alpha^z(q)}{\omega - q\Omega + i\eta} \tau_z^F + \frac{r_\alpha^+(q)e^{i\epsilon_q t}}{\omega - \epsilon_q - q\Omega + i\eta} \tau_+^F + \frac{r_\alpha^-(q)e^{-i\epsilon_q t}}{\omega + \epsilon_q - q\Omega + i\eta} \tau_-^F \right) \rho(t) (r_\alpha^z(k)\tau_z^F + r_\alpha^+(k)\tau_+^F e^{i\epsilon_q t} + r_\alpha^-(k)\tau_-^F e^{-i\epsilon_q t}) \right] + \text{h.c.} .
\end{aligned}$$

Next we perform the secular approximation, which means keeping in the above expression only the terms that oscillate slow compared to the dynamics of the qubit. Assuming non-zero $\epsilon_q \neq 0$ ($\epsilon_q = 0$ needs to be treated separately) and recalling that $-\Omega/2 < \epsilon_q < \Omega/2$, implies first that $q = -k$ in the above expressions. We end up with:

$$\begin{aligned}
\frac{d\rho(t)}{dt} &= -i \int d\omega \sum_\alpha J_\alpha(\omega) \sum_k \left[\left(\frac{|r_\alpha^z(k)|^2}{\omega + k\Omega + i\eta} \tau_z^F \tau_z^F + \frac{|r_\alpha^-(k)|^2}{\omega - \epsilon_q + k\Omega + i\eta} \tau_-^F \tau_+^F + \frac{|r_\alpha^+(k)|^2}{\omega + \epsilon_q + k\Omega + i\eta} \tau_+^F \tau_-^F \right) \rho(t) \right. \\
&\quad \left. - \left(\frac{|r_\alpha^z(k)|^2}{\omega + k\Omega + i\eta} \tau_z^F \rho \tau_z^F + \frac{|r_\alpha^-(k)|^2}{\omega - \epsilon_q + k\Omega + i\eta} \tau_-^F \rho \tau_-^F + \frac{|r_\alpha^+(k)|^2}{\omega + \epsilon_q + k\Omega + i\eta} \tau_+^F \rho \tau_+^F \right) \right] + \text{h.c.} . \quad (83)
\end{aligned}$$

Finally, neglecting the real part contribution in the above integrals, which represents the Lamb shift that slightly renormalizes the spectrum, the above expression can be cast in a Lindblad form⁶⁶:

$$\frac{d\rho(t)}{dt} = \Gamma_z \left(\tau_z^F \rho \tau_z^F - \frac{1}{2} \{ \tau_z^F \tau_z^F, \rho \} \right) + \Gamma_- \left(\tau_-^F \rho \tau_+^F - \frac{1}{2} \{ \tau_+^F \tau_-^F, \rho \} \right) + \Gamma_+ \left(\tau_+^F \rho \tau_-^F - \frac{1}{2} \{ \tau_-^F \tau_+^F, \rho \} \right), \quad (84)$$

with the rates showed in Eq. 31.

* sarathprem@magnet.ifpan.edu.pl

- ¹ A. Laucht, F. Hohls, N. Ubbelohde, M. F. Gonzalez-Zalba, D. J. Reilly, S. Stobbe, T. Schröder, P. Scarlino, J. V. Koski, A. Dzurak, C.-H. Yang, J. Yoneda, F. Kuemmeth, H. Bluhm, J. Pla, C. Hill, J. Salfi, A. Oiwa, J. T. Muhonen, E. Verhagen, M. D. LaHaye, H. H. Kim, A. W. Tsien, D. Culcer, A. Geresdi, J. A. Mol, V. Mohan, P. K. Jain, and J. Baugh, *Nanotechnology* **32**, 162003 (2021).
- ² L. Gyongyosi and S. Imre, *Computer Science Review* **31**, 51 (2019).
- ³ D. Loss and D. P. DiVincenzo, *Phys. Rev. A* **57**, 120 (1998).
- ⁴ C. Kloeffel and D. Loss, *Annual Review of Condensed Matter Physics* **4**, 51 (2013), <https://doi.org/10.1146/annurev-conmatphys-030212-184248>.
- ⁵ D. M. Zajac, T. M. Hazard, X. Mi, E. Nielsen, and J. R. Petta, *Phys. Rev. Appl.* **6**, 054013 (2016).
- ⁶ A. Chatterjee, P. Stevenson, S. D. Franceschi, A. Morello, N. P. de Leon, and F. Kuemmeth, *Nature Reviews Physics* **3**, 157 (2021).
- ⁷ G. Burkard, T. D. Ladd, J. M. Nichol, A. Pan, and J. R. Petta, "Semiconductor spin qubits," (2021).
- ⁸ R. J. Warburton, *Nature Materials* **12**, 483 (2013).
- ⁹ P. Harvey-Collard, B. D'Anjou, M. Rudolph, N. T. Jacobson, J. Dominguez, G. A. Ten Eyck, J. R. Wendt, T. Pluym, M. P. Lilly, W. A. Coish, M. Pioro-Ladrière, and M. S. Carroll, *Phys. Rev. X* **8**, 021046 (2018).
- ¹⁰ G. Zheng, N. Samkharadze, M. L. Noordam, N. Kalhor, D. Brousse, A. Sammak, G. Scappucci, and L. M. K. Vandersypen, *Nature Nanotechnology* **14**, 742 (2019).
- ¹¹ J. Yoneda, K. Takeda, T. Otsuka, T. Nakajima, M. R. Delbecq, G. Allison, T. Honda, T. Kodera, S. Oda, Y. Hoshi, N. Usami, K. M. Itoh, and S. Tarucha, *Nature Nanotechnology* **13**, 102 (2018).
- ¹² C. H. Yang, K. W. Chan, R. Harper, W. Huang, T. Evans, J. C. C. Hwang, B. Hensen, A. Laucht, T. Tanttu, F. E. Hudson, S. T. Flammia, K. M. Itoh, A. Morello, S. D. Bartlett, and A. S. Dzurak, *Nature Electronics* **2**, 151 (2019).
- ¹³ N. W. Hendrickx, W. I. L. Lawrie, L. Petit, A. Sammak, G. Scappucci, and M. Veldhorst, *Nature Communications* **11** (2020), 10.1038/s41467-020-17211-7.
- ¹⁴ X. Xue, M. Russ, N. Samkharadze, B. Undseth, A. Sammak, G. Scappucci, and L. M. K. Vandersypen, *Nature* **601**, 343 (2022).
- ¹⁵ A. Noiri, K. Takeda, T. Nakajima, T. Kobayashi, A. Sammak, G. Scappucci, and S. Tarucha, *Nature* **601**, 338 (2022).
- ¹⁶ M. T. Madzik, S. Asaad, A. Youssry, B. Joecker, K. M. Rudinger, E. Nielsen, K. C. Young, T. J. Proctor, A. D. Baczewski, A. Laucht, V. Schmitt, F. E. Hudson, K. M. Itoh, A. M. Jakob, B. C. Johnson, D. N. Jamieson, A. S. Dzurak, C. Ferrie, R. Blume-Kohout, and A. Morello, *Nature* **601**, 348 (2022).
- ¹⁷ V. N. Golovach, M. Borhani, and D. Loss, *Phys. Rev. B* **74**, 165319 (2006).
- ¹⁸ K. C. Nowack, F. H. L. Koppens, Y. V. Nazarov, and L. M. K. Vandersypen, *Science* **318**, 1430 (2007), <https://www.science.org/doi/10.1126/science.1148092>.
- ¹⁹ S. Nadj-Perge, S. M. Frolov, E. P. A. M. Bakkers, and L. P. Kouwenhoven, *Nature* **468**, 1084 (2010).
- ²⁰ A. Corna, L. Bourdet, R. Maurand, A. Crippa, D. Kotekar-Patil, H. Bohuslavskyi, R. Laviéville, L. Hutin, S. Barraud, X. Jehl, M. Vinet, S. De Franceschi, Y.-M. Niquet, and M. Sanquer, *npj Quantum Information* **4**, 6 (2018).
- ²¹ V. S. Pribiag, S. Nadj-Perge, S. M. Frolov, J. W. G. van den Berg, I. van Weperen, S. R. Plissard, E. P. A. M. Bakkers, and L. P. Kouwenhoven, *Nature Nanotechnology* **8**, 170 (2013).
- ²² A. Blais, A. L. Grimsmo, S. M. Girvin, and A. Wallraff, *Rev. Mod. Phys.* **93**, 025005 (2021).
- ²³ T. Bonsen, P. Harvey-Collard, M. Russ, J. Dijkema, A. Sammak, G. Scappucci, and L. M. K. Vandersypen, "Probing the jaynes-cummings ladder with spin circuit quantum electrodynamics," (2022).
- ²⁴ Z. Wang, E. Marcellina, A. R. Hamilton, J. H. Cullen, S. Rogge, J. Salfi, and D. Culcer, *npj Quantum Information* **7**, 54 (2021).
- ²⁵ S. Bosco, B. Hetényi, and D. Loss, *PRX Quantum* **2**, 010348 (2021).
- ²⁶ O. Malkoc, P. Stano, and D. Loss, *Phys. Rev. Lett.* **129**, 247701 (2022).
- ²⁷ H. Watzinger, J. Kukučka, L. Vukušić, F. Gao, T. Wang, F. Schäffler, J.-J. Zhang, and G. Katsaros, *Nature Communications* **9**, 3902 (2018).
- ²⁸ P.-A. Mortemousque, B. Jadot, E. Chanrion, V. Thimey, C. Bäuerle, A. Ludwig, A. D. Wieck, M. Urdampilleta, and T. Meunier, *PRX Quantum* **2**, 030331 (2021).
- ²⁹ C. P. Slichter, *Principles of magnetic resonance*, 2nd ed., Springer series in solid-state sciences ; v. 1 (Springer-Verlag, Berlin ;, 1978).
- ³⁰ P. Huang and X. Hu, *Phys. Rev. B* **88**, 075301 (2013).
- ³¹ P. S. Mundada, A. Gyenis, Z. Huang, J. Koch, and A. A. Houck, *Phys. Rev. Appl.* **14**, 054033 (2020).
- ³² Z. Huang, P. S. Mundada, A. Gyenis, D. I. Schuster, A. A. Houck, and J. Koch, *Phys. Rev. Appl.* **15**, 034065 (2021).
- ³³ A. Gandon, C. Le Calonnec, R. Shillito, A. Petrescu, and A. Blais, *Phys. Rev. Appl.* **17**, 064006 (2022).
- ³⁴ P. San-Jose, G. Zarand, A. Shnirman, and G. Schön, *Phys. Rev. Lett.* **97**, 076803 (2006).

³⁵ P. San-Jose, B. Scharfenberger, G. Schön, A. Shnirman, and G. Zarand, Phys. Rev. B **77**, 045305 (2008).

³⁶ M. Trif, P. Simon, and D. Loss, Phys. Rev. Lett. **103**, 106601 (2009).

³⁷ V. N. Golovach, M. Borhani, and D. Loss, Phys. Rev. A **81**, 022315 (2010).

³⁸ M. M. Wysokiński, M. Płodzień, and M. Trif, Phys. Rev. B **104**, L041402 (2021).

³⁹ G. De Chiara and G. M. Palma, Phys. Rev. Lett. **91**, 090404 (2003).

⁴⁰ A. Carollo, I. Fuentes-Guridi, M. F. m. c. Santos, and V. Vedral, Phys. Rev. Lett. **92**, 020402 (2004).

⁴¹ C. Lupo, P. Aniello, M. Napolitano, and G. Florio, Phys. Rev. A **76**, 012309 (2007).

⁴² R. Winkler, *Spin-orbit coupling effects in two-dimensional electron and hole systems*, Springer tracts in modern physics (Springer, Berlin, 2003).

⁴³ M. Trif, V. N. Golovach, and D. Loss, Phys. Rev. B **77**, 045434 (2008).

⁴⁴ M. Boissonneault, J. M. Gambetta, and A. Blais, Phys. Rev. A **79**, 013819 (2009).

⁴⁵ N. Didier, J. Bourassa, and A. Blais, Phys. Rev. Lett. **115**, 203601 (2015).

⁴⁶ B. Royer, A. L. Grimsmo, N. Didier, and A. Blais, Quantum **1**, 11 (2017).

⁴⁷ S. P. Harvey, C. G. L. Böttcher, L. A. Orona, S. D. Bartlett, A. C. Doherty, and A. Yacoby, Phys. Rev. B **97**, 235409 (2018).

⁴⁸ S. Bosco, P. Scarlino, J. Klinovaja, and D. Loss, Phys. Rev. Lett. **129**, 066801 (2022).

⁴⁹ M. S. Rudner and N. H. Lindner, “The floquet engineer’s handbook,” (2020).

⁵⁰ U. D. Giovannini and H. Hübener, Journal of Physics: Materials **3**, 012001 (2019).

⁵¹ Y. Aharonov and J. Anandan, Phys. Rev. Lett. **58**, 1593 (1987).

⁵² A. A. Reynoso, J. P. Baltanás, H. Saarikoski, J. E. Vázquez-Lozano, J. Nitta, and D. Frustaglia, New Journal of Physics **19**, 063010 (2017).

⁵³ A. Gandon, C. Le Calonnec, R. Shillito, A. Petrescu, and A. Blais, Phys. Rev. Appl. **17**, 064006 (2022).

⁵⁴ J. Hausinger and M. Grifoni, Phys. Rev. A **81**, 022117 (2010).

⁵⁵ S. Haroche and J. M. Raimond, *Exploring the Quantum: Atoms, Cavities, and Photons* (Oxford Univ. Press, Oxford, 2006).

⁵⁶ S. Bosco, P. Scarlino, J. Klinovaja, and D. Loss, Phys. Rev. Lett. **129**, 066801 (2022).

⁵⁷ C. Kloeffel, M. Trif, and D. Loss, Phys. Rev. B **84**, 195314 (2011).

⁵⁸ C. Kloeffel, M. Trif, P. Stano, and D. Loss, Phys. Rev. B **88**, 241405 (2013).

⁵⁹ K. D. Petersson, L. W. McFaul, M. D. Schroer, M. Jung, J. M. Taylor, A. A. Houck, and J. R. Petta, Nature **490**, 380 (2012).

⁶⁰ X. Mi, M. Benito, S. Putz, D. M. Zajac, J. M. Taylor, G. Burkard, and J. R. Petta, Nature **555**, 599 (2018).

⁶¹ A. A. Clerk, M. H. Devoret, S. M. Girvin, F. Marquardt, and R. J. Schoelkopf, Rev. Mod. Phys. **82**, 1155 (2010).

⁶² S. Kohler, Phys. Rev. Lett. **119**, 196802 (2017).

⁶³ M. Trif and P. Simon, Phys. Rev. Lett. **122**, 236803 (2019).

⁶⁴ A. V. Khaetskii and Y. V. Nazarov, Phys. Rev. B **61**, 12639 (2000).

⁶⁵ V. N. Golovach, A. Khaetskii, and D. Loss, Phys. Rev. Lett. **93**, 016601 (2004).

⁶⁶ H. P. Breuer and F. Petruccione, *The theory of open quantum systems* (Oxford University Press, Great Clarendon Street, 2002).

⁶⁷ A. J. Leggett, S. Chakravarty, A. T. Dorsey, M. P. A. Fisher, A. Garg, and W. Zwerger, Rev. Mod. Phys. **59**, 1 (1987).

⁶⁸ R. Blattmann, P. Hänggi, and S. Kohler, Phys. Rev. A **91**, 042109 (2015).

⁶⁹ C. F. Roos, New Journal of Physics **10**, 013002 (2008).

⁷⁰ P. H. Leung, K. A. Landsman, C. Figgatt, N. M. Linke, C. Monroe, and K. R. Brown, Phys. Rev. Lett. **120**, 020501 (2018).

⁷¹ S. Bosco, M. Benito, C. Adelsberger, and D. Loss, Phys. Rev. B **104**, 115425 (2021).

⁷² C. Kloeffel, M. J. Rančić, and D. Loss, Phys. Rev. B **97**, 235422 (2018).

⁷³ S. Bosco, B. Hetényi, and D. Loss, PRX Quantum **2**, 010348 (2021).

⁷⁴ S.-S. Li, J.-B. Xia, Z. L. Yuan, Z. Y. Xu, W. Ge, X. R. Wang, Y. Wang, J. Wang, and L. L. Chang, Phys. Rev. B **54**, 11575 (1996).

⁷⁵ K. Snizhko, R. Egger, and Y. Gefen, Phys. Rev. B **100**, 085303 (2019).

⁷⁶ M. Westig, B. Kubala, O. Parlavecchio, Y. Mukharsky, C. Altimiras, P. Joyez, D. Vion, P. Roche, D. Esteve, M. Hofheinz, M. Trif, P. Simon, J. Ankerhold, and F. Portier, Phys. Rev. Lett. **119**, 137001 (2017).